COMPOSITES OF CARBON NANOTUBES

By

MAXIM NIKOLAEVICH TCHOUL

Bachelor of Science
Belarus State University
Minsk, Belarus
1991

Master of Science
Belarus State University
Minsk, Belarus
1992

Submitted to the Faculty of the
Graduate College of the
Oklahoma State University
in partial fulfillment of
the requirements for
the Degree of
DOCTOR OF PHILOSOPHY
May, 2008

COMPOSITES OF CARBON NANOTUBES

Dissertation Approved:

Dr. Warren T. Ford

Dissertation Adviser

Dr. K. Darrell Berlin

Dr. Legrande M. Slaughter

Dr. Ziad El Rassi

Dr. James P. Wicksted

Dr. A. Gordon Emslie

Dean of the Graduate College

PREFACE

Carbon nanotubes, a new synthetic form of carbon, are hollow tubes from 0.4 to tens of nanometers in diameter composed of carbon atoms. These tiny tubes have been a subject of a close interest of researchers worldwide due to their unique properties. For example, individual carbon nanotubes can work as nanometer scale transistors and wires, which makes possible constructing electronic devices compared to the size of single molecules. Being a 100 times stronger and 5 times lighter than steel, carbon nanotubes can be used as reinforcement to produce strong and light-weight composites. However, nanotubes mix poorly with other compounds as well as have a low adhesion to anything other than themselves, which prevents utilizing this material at its full advantage. This problem is being solved by modifying the surface of nanotubes with different molecules. As of today, numerous methods to overcome the immiscibility of carbon nanotubes have been found, although many of them are complicated and may never be used on a large scale. In this work several easy and potentially scalable methods were chosen for the incorporation of carbon nanotubes with polymers and their efficiency was studied toward producing electrically conductive composites. Such composites can be used in production of sensors and electrostatic dissipative materials. The percolation threshold, a minimum content of nanotubes needed to conduct the electric current through the sample, was used as a measure of efficiency of each method. Single-walled carbon nanotubes produced by different techniques were used to

compare their ability to disperse in polymers. The results of this study will assist engineers in development of new composite materials with carbon nanotubes.

ACKNOWLEDGEMENTS

First of all, I would like to express my gratitude to my Adviser, Professor Warren T. Ford, whose contribution to my research is hard to overestimate. His help and guidance along with providing us students with a great deal of freedom made us become confident and independent researchers.

I am thankful to the members of my Adviser Committee, Professors K. Darrell Berlin, Ziad El Rassi, Legrande M. Slaughter and James P. Wicksted for their help and counseling during my study.

I would like to thank my collaborators, Professors Daniel E. Resasco and Brian P. Grady from the School of Chemical, Biological and Materials Engineering, University of Oklahoma, from whom I have learned a lot. Raman experiments in Chapter IV have been done in the group of Prof. D. E. Resasco by Dr. Giulio Lolli. All the electrical conductivity measurements presented in Chapter V have been done in the group of Prof. B. P. Grady by Mr. Israel Chavez-Sumarriva and preliminary measurements not included in this dissertation have been done by Ms. Mai Ha. Raman spectroscopy analyses presented in Chapters II and III have been carried out in the group of Prof. J. P. Wicksted by Dr. Mohammed Gheith, Dr. Charles Blackledge and Mr. Deok Jin Yu. Shimadzu TGA-50 termogravimetric analyzer was provided by Prof. L. M. Slaughter. Heat press was provided by Prof. J. C. Hanan from the School of Mechanical and Aerospace Engineering OSU. Samples of CoMoCat SWNT were provided by Southwest

Nanotechnology Inc., Norman, OK. Samples of PLV SWNT were provided by Dr. Sivaram Arepalli from JSC NASA, Houston, TX.

I thank Dr. Susheng Tan from the OSU Microscopy Lab for his help with SEM and AFM microscopy. I would also like to thank the former members of our group Dr. Shuhui Qin and Mr. Xiaoming Jiang, for valuable discussions that helped me make lots of shortcuts along my research.

I wish to thank my first adviser at the OSU, Professor Nicholas A. Kotov, who helped me during my first days in the USA, as well as the former members of the Prof. Kotov's group, Dr. Vladimir A. Sinani and Dr. Arif A. Mamedov, with whom I started my research on carbon nanotubes.

And last but not least, I want to express my gratitude to my precious wife Oksana. Without her support and sacrifice I would probably never go far.

TABLE OF CONTENTS

LIST OF TABLES

Chapter III

Chapter IV

Chapter V

LIST OF FIGURES

Chapter II

Figure Page

Chapter III

Figure Page

Chapter IV

Figure Page

Chapter V

Figure Page

LIST OF SCHEMES

Chapter II

Chapter III

CHAPTER I
PROPERTIES AND PROSPECTIVE APPLICATIONS OF CARBON NANOTUBES

Introduction

Carbon is one of the most abundant elements in the universe.[1] A unique ability of carbon atoms to form strong bonds not only with other elements but also with themselves account for a tremendous variety of carbon compounds in nature. Because of this property, the idea of existence of molecules composed only of carbon atoms has occupied scientists for a long time. Although the possibility of formation of such structures has been predicted theoretically in 1973,[2] it was not until 1985 when the first spherical molecules containing 24 to 70 atoms of carbon had been obtained experimentally.[3,4] The name "fullerenes" was given to these compounds after the American architect R. Buckminster Fuller. Following the discovery of carbon nanotubes, a cylindrical analogue of fullerenes, by Iijima in 1991[5] this type of structures was recognized as a new allotropic form of carbon.

Carbon atoms in nanotubes exist in the sp^2 hybridized form, composing a hexagonal grid rolled into a cylinder, so that these structures are often described as "rolled-up graphene sheets,[6,7] although this is not the way they are formed. Carbon nanotubes grow on a metal catalyst in a grass-like fashion using carbon generated either by vaporization of graphite by laser[8] or electric arc[5] or by disproportionation of

carbon monoxide at high temperature.[9] Other methods include pyrolysis of methane or methanol in the presence of a catalyst.[10,11] Carbon nanotubes can be both single-walled and multi-walled. The latter consist of several coaxial layers inserted into each other. In the present work, I will discuss only single-walled carbon nanotubes (SWNT) so the term "single-walled" in most cases will be omitted.

Physical properties of carbon nanotubes. Physical properties of carbon nanotubes are primarily defined by their chiral indexes n and m, which indicate the direction of "rolling" of the graphene sheet as well as the diameter of a tube.[7,12] Due to the quantum confinement, the electron orbitals in a nanotube are associated in bands that are symmetrically located above and below the Fermi level.[6] However, the nanotubes for which (n-m) = 3q, where q is integer, possess some electron density at the Fermi level, allowing metallic type of electrical conductivity for these tubes which are therefore called "metallic" while the others are called "semiconducting".[7,13]

The distance between bands on the energy scale is defined by chiral indexes. The electron transition between the bands results in specific absorption of light in the region between 300 and 1800 nm for most nanotubes.[14] Metallic tubes exhibit a single peak corresponding to M_{11} transition and semiconducting tubes reveal two peaks due to S_{11} and S_{22} transitions. Strong absorption of carbon nanotubes in the near-infrared part of the spectra holds promise in utilizing this material for the photoinduced destruction of cancer cells in the human body.[15]

The presence of two bands in the semiconducting SWNT makes possible the fluorescence of these nanotubes in the near-infrared area of the spectra.[16] Fluorescence is normally observed for individually dispersed nanotubes, because one metallic nanotube

in a bundle quenches the fluorescence of semiconducting nanotubes. Due to such an effect nanotubes can be used as fluorescent labels for the imaging in biology, since most biological tissues are transparent to the NIR light.[17]

Carbon nanotubes as nanometer size semiconductors are actively explored toward applications in the nanoscale electronic devices. Fabrication of a logic circuit and a ring oscillator based on a single SWNT by the researchers from IBM demonstrated that electronic devices on the nanometer scale can be produced with carbon nanotubes.[18] SWNT also show competitive characteristics as field effect transistors[19] as well as materials for flat panel displays.[20]

Electrical transport in carbon nanotubes shows ballistic conductivity with quantum behavior.[21] The resistance of the individual single-walled metallic nanotubes is independent on their length for tubes under 1 μm, whereas the semiconducting nanotubes have a series of large barriers to conduction along their length.[22] Resistance of individual metallic tubes, measured by Skakalova at al,[23] was found to be about one order of magnitude lower than that of semiconducting tubes. Therefore, metallic tubes carry most of the current in bulk carbon nanotube material.

Tensile strength of individual single-walled carbon nanotubes was found to be between 22 and 55 GPa, depending on the applied method, and the Young's modulus reached the value of 1.25 TPa.[24] Such mechanical properties make nanotubes the strongest synthetic material ever known. That's why CNT is the most considered material for the "space elevator" idea to create the physical connection between the ground and a space orbiter.[25] Unfortunately, the use of the full advantage of the high mechanical strength of nanotubes is limited by a number of factors. First is the poor miscibility of

nanotubes with other materials and there are also defects in the tubes.[26] The strongest SWNT composite created so far had the tensile strength of about 1.8 GPa while containing 60% of SWNT in polyvinyl alcohol.[27]

Chemical properties of carbon nanotubes. Carbon atoms in nanotubes exist in the sp^2 hybridization state and, as in graphite, are located at equal distance from each other, which at some point resembles polyaromatic compounds. However, in most chemical reactions carbon nanotubes exhibit properties typical for alkenes. For example, reaction with organic peroxides results in addition of the in-situ generated radicals to nanotubes.[28] Reaction with sec-butyllithium leads to an addition to SWNT and formation of carbanions on their surface.[29] Carbon nanotubes undergo fluorination and hydrogenation in which fluorine and hydrogen covalently attach to carbon.[30] Fluorinated nanotubes become capable of reacting with Grignard reagents and alkyllithium to graft different functionalities on the surface.[30]

Reactions of carbon nanotubes with strong oxidants, such as concentrated nitric and sulfuric acids, result in oxidation of some carbon atoms into carbonyls and carboxyls.[31] The reactivity of the SWNT toward oxidation is inversely related to their diameter due to the increased strain in the small tubes.[32] Oxidation of carbon nanotubes is a widely used procedure for functionalization of this material, since addition of carboxylic groups to the surface opens vast possibilities for further chemistry.[33]

Nanotubes have been found to participate in Diels-Alder[34] and dipolar cycloaddition[35] reactions in which they act as a dienophile but not as a diene. Addition of carbenes[36] and osmium tetroxide[37] has also been reported which are typical reactions for

alkenes. The Bingel reaction, which is specific for fullerenes, is possible for carbon nanotubes as well.[38]

Composite materials of carbon nanotubes. The plastics industry is the main area where carbon nanotubes are so far being commercialized. According to the business report by Global Industry Analysts, the global market for the CNT composites was worth $43 million in 2006, which was more than 80% of the entire CNT industry.[39] In the next 5 years this sector is expected to grow by the factor of 10 to reach $451.2 million net worth by 2011. Research on polymeric composites of CNT experiences growth as well. According to the SciFinder publication statistics, the share of papers on this subject has increased from 1 % in 2000 to 5 % in 2007 of total number of publications on carbon nanotubes.[40]

Addition of carbon nanotubes into polymers increases tensile and compressive strength and tensile modulus,[41] which is useful for manufacturing of strong and lightweight construction materials. Electrical conductivity of polymers increases over several orders of magnitude by addition of 0.1 – 1 % of SWNT.[42] Polymeric composites of CNT show piezoresistivity,[43] non-linear I-V characteristics,[44] and optomechanical response[45] which offers possibility for developing new sensors and actuators. At the same time, carbon nanotubes are poorly miscible within polymers and generally insoluble in solvents, posing a challenge for utilizing this material at its full advantage. Therefore, the main objective of the present research is to investigate the methods for the efficient incorporation of nanotubes into polymeric composites.

References

(1) Lide, D. R., Ed. *CRC Handbook of Chemistry and Physics*; 85 ed.; CRC Press: Boca Raton, FL, 2005.

(2) Bochvar, D. A.; Galpern, E. G. *Dokl. Acad. Nauk USSR* **1973**, *209*, 610.

(3) Kroto, H. W.; Heath, J. R.; O'Brien, S. C.; Curl, R. F.; Smalley, R. E. *Nature* **1985**, *318*, 162.

(4) Zhang, Q. L.; O'Brien, S. C.; Heath, J. R.; Liu, Y.; Curl, R. F.; Kroto, H. W.; Smalley, R. E. *J. Phys. Chem.* **1986**, *90*, 525.

(5) Iijima, S. *Nature* **1991**, *354*, 56.

(6) Dresselhaus, M. S. *Nature* **1998**, *391*, 19.

(7) Hamada, N.; Sawada, S.; Oshiyama, A. *Phys. Rev. Lett.* **1992**, *68*, 1579.

(8) Thess, A.; Lee, R.; Nikolaev, P.; Dai, H.; Petit, P.; Robert, J.; Xu, C.; Lee, Y. H.; Kim, S. G.; Rinzler, A. G.; Colbert, D. T.; Scuseria, G. E.; Tomanek, D.; Fischer, J. E.; Smalley, R. E. *Science* **1996**, *273*, 483.

(9) Dai, H.; Rinzler, A. G.; Nikolaev, P.; Thess, A.; Colbert, D. T.; Smalley, R.E. *Chem. Phys. Lett.* **1996**, *260*, 471.

(10) Kong, J.; Soh, H. T.; Cassell, A. M.; Quate, C. F.; Dai, H. J. *Nature* **1998**, *395*, 878.

(11) Maruyama, S.; Kojima, R.; Miyauchi, Y.; Chiashi, S.; Kohno, M. *Chem. Phys. Lett.* **2002**, *360*, 229.

(12) Bachilo, S. M.; Strano, M. S.; Kittrell, C.; Hauge, R. H.; Smalley, R. E.; Weisman, R. B. *Science* **2002**, *298*, 2361.

(13) Mintmire, J. W.; Dunlap, B. I.; White, C. T. *Phys. Rev. Lett.* **1992**, *68*, 631.

(14) Jorio, A.; Saito, R.; Hertel, T.; Weisman, R. B.; Dresselhaus, G.; Dresselhaus, M. S. *MRS Bulletin* **2004**, *29*, 276.

(15) Kam, N. W. S.; O'Connell, M.; Wisdom, J. A.; Dai, H. *PNAS* **2005**, *102*, 11600.

(16) O'Connell, M. J.; Bachilo, S. M.; Huffman, C. B.; Moore, V. C.; Strano, M. S.; Haroz, E. H.; Rialon, K. L.; Boul, P. J.; Noon, W. H.; Kittrell, C.; Ma, J.; Hauge, R. H.; Weisman, R. B.; Smalley, R. E. *Science* **2002**, *297*, 593.

(17) Leeuw, T. K.; Reith, R. M.; Simonette, R. A.; Harden, M. E.; Cherukuri, P.; Tsyboulski, D. A.; Beckingham, K. M.; Weisman, R. B. *Nano Lett.* **2007**, *7*, 2650.

(18) Chen, Z.; Appenzeller, J.; Lin, Y.-M.; Sippel-Oakley, J.; Rinzler, A. G; Tang, J.; Wind, S. J.; Solomon, P. M; Avouris, P. *Science* **2006**, *311*, 1735.

(19) Martel, R.; Schmidt, T.; Shea, H. R.; Hertel, T.; Avouris, P. *Appl. Phys. Lett.* **1998**, *73*, 2447.

(20) Wang, Q. H.; Setlur, A. A.; Lauerhaas, J. M.; Dai, J. Y.; Seelig, E. W.; Chang, R. P. H. *Appl. Phys. Lett.* **1998**, *72*, 2912.

(21) Frank, S.; Poncharal, P.; Wang, Z. L.; de Heer, W. A. *Science* **1998**, *280*, 1744.

(22) Bachtold, A.; Fuhrer, M. S.; Plyasunov, S.; Forero, M.; Anderson, E. H.; Zettl, A.; McEuen, P. L. *Phys. Rev. Lett.* **2000**, *84*, 6082.

(23) Skakalova, V.; Kaiser, A. B.; Woo, Y. S.; Roth, S. *Phys. Rev. B* **2006**, *74*.

(24) Qian, D.; Wagner, G. J.; Liu, W. K.; Yu, M.-F.; Ruoff, R. S. *Appl. Mech. Rev.* **2002**, *55*, 495.

(25) Pugno, N. M. *J. Phys.: Condens. Matter* **2006**, *18*, S1971.

(26) Salvetat, J.-P.; Bhattacharyya, S.; Pipes, R. B. *J. Nanosci. Nanotechnol.* **2006**, *6*, 1857.

(27) Dalton, A. B.; Collins, S.; Munoz, E.; Razal, J. M.; Ebron, V. H.; Ferraris, J. P.; Coleman, J. N.; Kim, B. G.; Baughman, R. H. *Nature* **2003**, *423*, 703.

(28) Ying, Y.; Saini, R. K.; Liang, F.; Sadana, A. K.; Billups, W. E. *Organic Lett.* **2003**, *5*, 1471.

(29) Chen, S.; Shen, W.; Wu, G.; Chen, D.; Jiang, M. *Chem. Phys. Lett.* **2005**, *402*, 312.

(30) Hirsch, A.; Vostrowsky, O. *Top Curr Chem* **2005**, *245*, 193.

(31) Zhang, J.; Zou, H.; Qing, Q.; Yang, Y.; Li, Q.; Liu, Z.; Guo, X.; Du, Z. *J. Phys. Chem. B* **2003**, *107*, 3712.

(32) Tchoul, M. N., Ford, W. T.; Lolli, G.; Resasco, D. E.; Arepalli, S. *Chem. Mater.* **2007**, *19*, 5765.

(33) Lin, Y.; Meziani, M. J.; Sun, Y.-P. *J. Mater. Chem.* **2007**, *17*, 1143.

(34) Menard-Moyon, C.; Dumas, F.; Doris, E.; Mioskowski, C. *J. Am. Chem. Soc.* **2006**, *128*, 14764.

(35) Tagmatarchis, N.; Prato, M. *J. Mater. Chem.* **2004**, *14*, 437.

(36) Hu, H.; Zhao, B.; Hamon, M. A.; Kamaras, K.; Itkis, M. I.; Haddon R. C. *J. Am. Chem. Soc.* **2003**, *125*, 14893.

(37) Cui, J.; Burghard, M.; Kern, K. *Nano Letters* **2003**, *3*, 613.

(38) Coleman, K. S.; Bailey, S. R.; Fogden, S.; Green, M. L. H. *J. Am. Chem. Soc.* **2003**, *125*, 8722.

(39) *Carbon nanotubes: A global strategic business report*, Global Industry Analysts Inc: San Jose, CA, 2007.

(40) "SciFinder literature analysis by the keywords "carbon nanotubes", "polymer" and composite", performed on 10/31/2007

(41) Coleman, J. N.; Khan, U.; B.; Blau, W. J.; Grin'ko, Y. K. *Carbon* **2006**, *44*, 1624.

(42) Winey, K. I.; Kashiwagi, T.; Mu, M. *MRS Bulletin* **2007**, *32*, 348.

(43) Regoliosi, P.; Brunetti, F.; Reale, A.; Di Carlo, A.; Tamburri, E.; Orlanducci, E.; Terranova, M. L.; Lugli P. *Proc. SPIE* **2005**, *5838*, 77.

(44) Pradhan, B.; Batabyal, S. K.; Pal, A. J. *J. Phys. Chem. B* **2006**, *110*, 8274.

(45) Lu, S. X.; Panchapakesan, B. *Nanotechnology* **2007**, *18*, 305502.

CHAPTER II

GRAFTING OF POLY(VINYLBENZYL TRIMETHYLAMMONIUM CHLORIDE) TO SINGLE-WALLED CARBON NANOTUBES

Abstract

Single-walled carbon nanotubes were functionalized by poly((vinylbenzyl)trimethylammonium chloride) (PVBTMA) through the in-situ radical polymerization. The resulting aqueous dispersions were stable for as long as 7 months without precipitation and consisted principally of individual carbon nanotubes and small bundles, according to atomic force microscopy tests. The material, after purification, contained 34% of a polymer by weight. Raman scattering spectra of the material, compared with those of pristine SWNT, suggested covalent bonding of polymer chains to the nanotube surface. Small changes in Raman and UV-VIS-NIR spectra of the SWNT after functionalization indicated that electronic structure of nanotubes was not disrupted significantly. Ability of the synthesized material to undergo layer-by-layer deposition with negatively charged moieties has been demonstrated.

Introduction

Layer-by-layer deposition (LBL) is a versatile method of producing composite materials via the consecutive deposition of layers of different moieties from aqueous solutions driven by electrostatic interaction.[1] Great advantages of this method include the ability to combine together the materials that cannot be combined by any other methods as well as the ability to produce a composite with desired properties by controlling the structure during the deposition. A number of new materials containing carbon nanotubes has been developed recently using LBL. Combination of SWNT with porphyrins allowed the photovoltaic composites with high quantum yield.[2] Scaffolds for healing nerve tissue have been produced by co-deposition of nanotubes and poly(acrylic acid).[3] The multilayer films of SWNT with polyaniline and polyvinyl alcohol produced by LBL exhibited dependence of electrical resistance on pH and mechanical stress, which makes them applicable as strain and corrosion sensors.[4] Incorporation of oxidized nanotubes with poly(ethylene imine) using layer-by-layer deposition increased the tensile strength of the composite by a factor of 20 with respect to the neat polymer.[5] The nanotube loading in this material was 50 % by weight.

In order to be used in layer-by-layer deposition, carbon nanotubes have to be dispersed in water. The most common approach to dispersing nanotubes is the use of surfactants.[6] However, due to the adsorption-desorption equilibrium, the presence of free surfactant in solution is required to keep it adsorbed on the surface of nanotubes. The more surfactant is added, the higher the concentration of suspended nanotubes.[7] Hence, the use of the surfactant-stabilized nanotube dispersions in LBL will result in the undesired addition of surfactant in the final composite.

Covalent functionalization of nanotubes can solve the problem of adsorption by permanently binding of the desired moieties to the surface of SWNT. Either positive or negative charge can be created on nanotubes by addition of the compounds containing amine or carboxyl groups via different functionalization procedures.[8,9] In this approach, one unit of charge per one covalent bond with the nanotube is usually created. Therefore, in order to obtain the sufficient charge on the tube, its surface has to be heavily functionalized, which alters electronic and mechanical properties of the nanotubes.[10,11] To avoid this problem, nanotubes can be functionalized with polyelectrolytes, in which case as many as 100 units of charge can be permanently attached to a nanotube by creating only a single bond with a carbon atom of the tube. Such idea was utilized in functionalization of SWNT with poly(sodium styrenesulfonate),[12] where the resulting composites formed aqueous dispersions stable for several months, and the electronic properties of the nanotubes were practically unchanged.

The objective of this work was to covalently graft a cationic polyelectrolyte to carbon nanotubes in order to provide a water-soluble composite of nanotubes with preserved electronic properties for use in layer-by-layer process. Some applications of the multilayer composites especially require the positive charge on nanotubes. For example, for the tissue implants, the surface of the composite has to possess positive charge in order for the negatively charged cell membrane to bind to the SWNT fibers.[3]

Experimental

Materials and Methods. Single-walled carbon nanotubes in the form of a 22 mg/g aqueous gel were obtained from Southwest Nanotechnologies Inc., Norman, OK. The

VBTMA-Cl monomer (mixture of meta- and para- isomers) was purchased from Aldrich. The VA-044 initiator (2,2'-azobis[2-(2-imidazolin-2-yl)propane] dihydrochloride) was obtained from WAKO Pure Chemical Industries Ltd. Bath sonication was carried out in a FS20 ultrasonic cleaner 70W 42KHz (Fisher Scientific). Low speed centrifugation of SWNT/polymer dispersions was performed on an IEC EXD centrifuge (IEC, Needham, MA). Ultracentrifugation was performed on a Beckman L8-70M centrifuge with Ti75 rotor. Ultrafiltration was performed in an Amicon-8400 ultrafiltration cell (Millipore) under 10 psi pressure. Atomic force micrographs were obtained using a Multimode Nanoscope IIIa SPM (Digital Instruments, Santa Barbara, CA) operating in the tapping mode. The samples were prepared by applying a drop of suspension on a mica chip for 1 min, followed by rinsing with water and drying in nitrogen flow. The Raman measurements were carried out using a Coherent Argon-ion laser operating at an excitation wavelength of 514.5 nm. The laser power was 1.0 mW; the time for a scan was 60 s. The back-scattered light was analyzed using a SPEX 500M single grating spectrometer with a liquid nitrogen cooled charge coupled detector (CCD). The samples were prepared by applying a drop of a suspension on a clean silicon surface followed by drying at 75 °C to yield a solid surface coating. Such a procedure was repeated 10 times for each sample. UV-VIS spectroscopy in the wavelength range of 190 – 1100 nm was performed on a HP 8453 spectrophotometer (Hewlett Packard). Thermogravimetric analyses were performed using a TGA50/50H analyzer (Shimadzu) in nitrogen atmosphere at a scan rate of 10 °C/min.

In-situ Polymerization of VBTMACl and SWNT. A 100 mL Schlenk flask containing 4.0 g of VBTMACl monomer, 40 mg of carbon nanotubes and 65 mL of deionized water

were sonicated for 30 min, followed by stirring for 4 h. Then, 48 mg of VA-044 was added, and the mixture was degassed by vacuum pump and refilled with nitrogen 3 times. The flask was sealed under vacuum, and the synthesis was carried out in a thermostated oil bath at 75 °C with stirring. After 48 h, the reaction was stopped by cooling to room temperature and opening the flask to air.

The mixture was diluted to 500 mL with water, bath sonicated for 1 h, and centrifuged at 5000g for 6 h. The homogenous black supernatant was removed. The black sediment was redispersed in water by stirring, and the procedure was repeated two more times. The combined supernatants were concentrated by ultrafiltration through a 0.45 μm cellulose acetate membrane until the volume decreased to 100 mL. The concentrated suspension was centrifuged at 200000g for 2 h in order to precipitate SWNT-PVBTMACl. The transparent solution of residual free polymer was decanted. The precipitate was redispersed in water, and the procedure was repeated two more times. Part of the final black precipitate was vacuum dried at 100 °C for 48 h for TGA, and the rest was dispersed in 100 mL of water at 0.2 g/L by 30 min of bath sonication.

Synthesis of PVBTMACl. A 100 mL Schlenk flask containing a solution of 4.0 g of VBTMACl in 65 mL of deionized water was degassed by vacuum pump and refilled with nitrogen 3 times. The flask was sealed under vacuum, and the synthesis was carried out in a thermostated oil bath at at 75 °C with stirring. After 48 h, the reaction was stopped by cooling to room temperature and opening the flask to air. The polymer was isolated by rotary evaporation under vacuum followed by drying in vacuum for 12 h at room temperature.

Dispersion of SWNT in PVBTMACl. A 2 g/L aqueous solution of the PVBTMACl and 4 mg of SWNT were dispersed in 50 mL of this solution by bath sonication for 1 h followed by centrifugation at 5000g for 6 h. The supernatant was decanted and the sample for optical absorption was taken. The rest of the material was subjected to 3 cycles of ultracentrifugation, according to the procedure described above, for the purification of the grafted SWNT. The final SWNT material was redispersed in 20 mL of water by 30 min bath sonication.

Layer-by-layer Assembly. A 0.05 g/L aqueous solution of purified SWNT-PVBTMACl was used for the deposition. SWNT grafted with poly(sodium styrenesulfonate) (SWNT-PSS) were synthesized according to the published procedure[12] and used in a form of the 0.05 g/L aqueous solution. Poly(acrylic acid) (PAA), M_W = 450,000 and poly(diallyldimethyl ammonium chloride) (PDDA), M_W = 400,000, were purchased from Aldrich and used in the form of 10 g/L aqueous solutions with pH adjusted to 7.0. The 3x5" microscopic glass substrate was cleaned by a 15 min bath sonication in acetone, followed by 15 min boiling in sodium carbonate, followed by rinsing in water. The clean slide was coated with a layer of PDDA by immersing it in the solution of this polymer for 15 min, followed by washing with water 3x1 min. The SWNT-PSS vs. SWNT-PVBTMA LBL film was made by subsequent immersing the slide in the solution of each nanotube material for 60 min, followed by washing with water 2x1 min and immersing in the solution of the other nanotube material. The SWNT-PVBTMA vs. PAA LBL film was made by subsequent immersing of the slide in the PAA solution for 10 min followed by washing with water 3x1.5 min and immersing the slide in the SWNT-PVBTMACl solution for 60 min, followed by washing with water 2x1 min. The slide was dried in a

gentle nitrogen flow before being immersed in the SWNT or PAA solutions. The growth of the film was monitored by measuring the optical absorption of the slide at 400 nm. The 60 min deposition time was chosen by comparing the various times in the SWNT versus PSS experiments. The absorption of the film increased with the deposition time under 60 min, and no noticeable increase was observed for times longer than 60 min.

Results and Discussion

The synthetic procedure for grafting PVBTMA to SWNT is presented in Scheme 1.

Scheme 1. Experimental procedure.

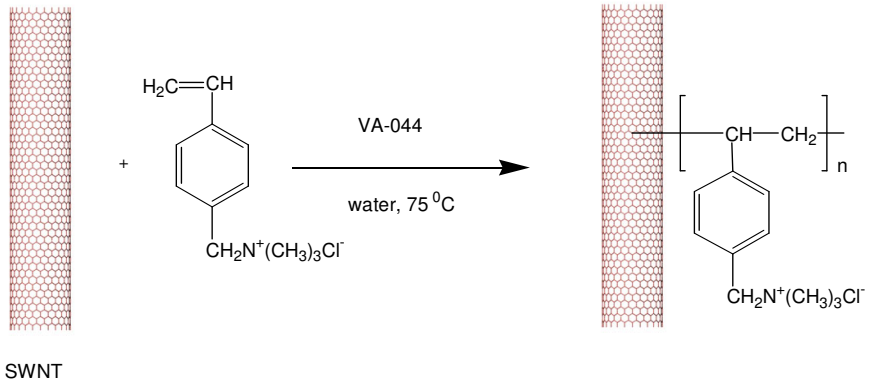

Figure 1 compares the TGA analysis of the purified SWNT-PVBTMACl composite alone with the TGA of pristine SWNT and pure polymer, which allows the estimation of the SWNT:PVBTMACl ratio in the composite to be 66:34 by weight. Recalculated into molecular weight this ratio gives one monomer unit per 28 atoms of carbon of the SWNT. This ratio is close to that for the highly functionalized SWNT from the reaction with in-situ generated diazonium compounds.[10] Unlike those materials which

lose all the band features in the UV-VIS spectra, this material has its spectrum practically unchanged, as seen in Figure 2. Low changes in the UV-VIS spectra indicate that useful properties of carbon nanotubes, such as electrical conductivity, are preserved in the SWNT-PVBTMACl material. A 15 nm red shift in the maximum of the S_{11} peak for the [6,5] nanotube in the functionalized sample, compared to the sample of dispersed SWNT can be explained by interaction of the SWNT surface with water due to its low coverage with polymer.[6] The grafted sample used for the spectral analysis contained 0.1 g/L SWNT and 0.05 g/L of the polymer, compared to the 0.08 and 2.0 g/L for the dispersed sample, respectively.

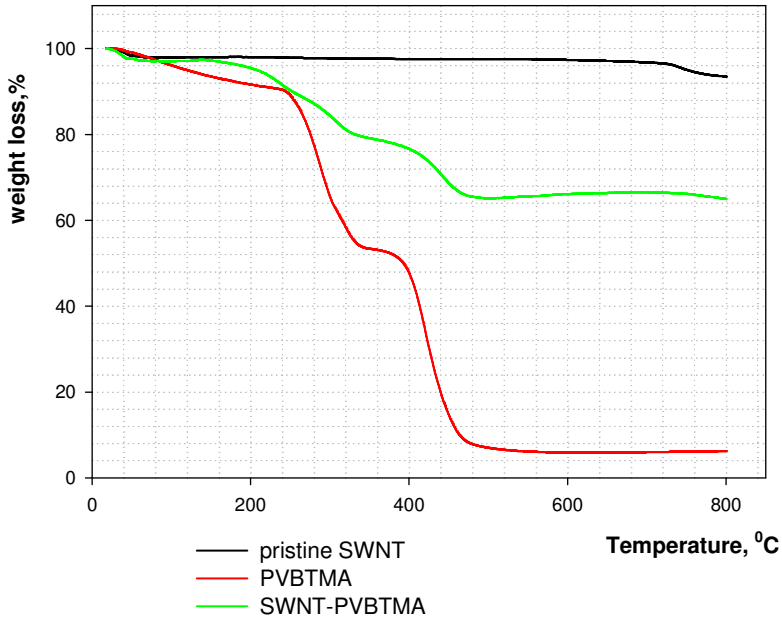

Figure 1. TGA analysis of the pristine SWNT, PVBTMA and SWNT-PVBTMA grafted material in a nitrogen atmosphere.

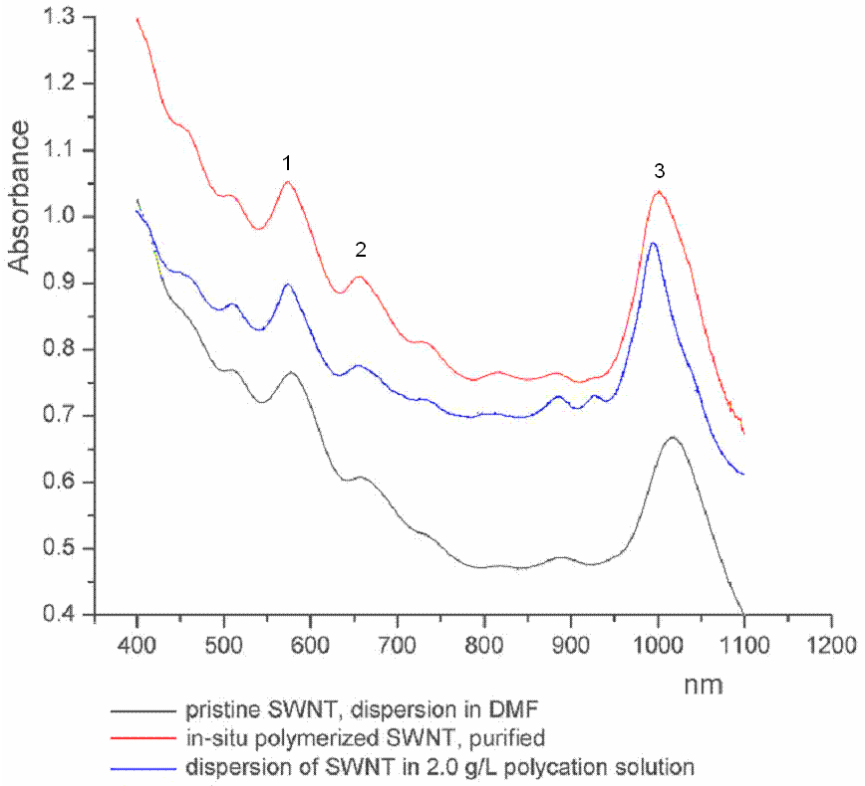

Figure 2. UV-VIS absorption of the SWNT-PVBTMA in water, dispersion of SWNT in the 2 g/L solution of the PVBTMA and pristine SWNT in DMF. The peaks #1 and #3 correspond to the S_{22} and S_{11} transitions for the [6,5] nanotube, the peak #2 corresponds to the S_{22} transition for the [7,5] nanotube.

Small changes in the optical absorption spectra correlate with the small changes in the Raman spectra of the SWNT after functionalization, as seen in Figure 3. The intensity of the D-band (I_D) at 1320 cm^{-1} (arising due to defects in the structure of the nanotube sidewall) in respect to the intensity of the G-band (I_G) 1590 cm^{-1} (corresponding to the stretching vibrations of the sp^2 carbons) is used as an estimation of the fraction of the sp^3 hybridized carbon atoms.[13] The I_D/I_G ratio is increased from 0.1 to 0.13 after the in-situ polymerization due to addition of some polymer molecules to nanotubes. Such an

increase is very low compared to other functionalization procedures reported in literature, where the the I_D:I_G ratio typically increases by the factor of 5-20.[9,10,14]

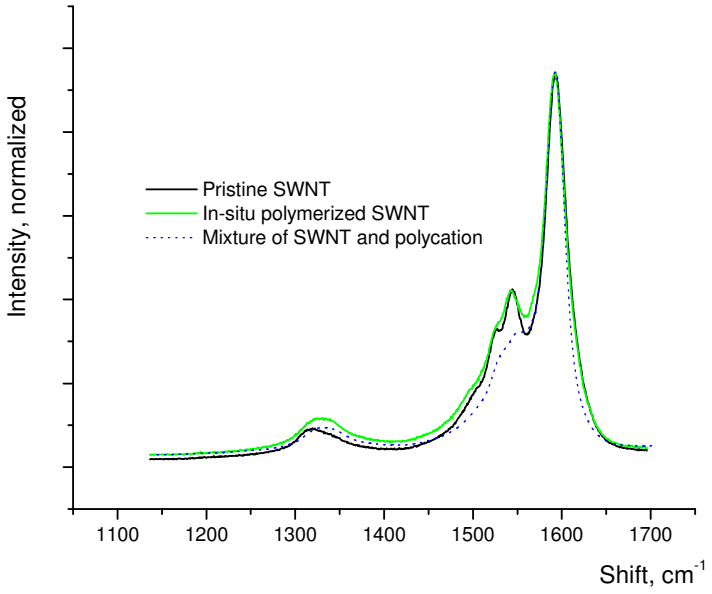

Figure 3. Raman spectra of the pristine SWNT, SWNT-PVBTMA and SWNT dispersed with PVBTMA.

Despite its low weight fraction, the attached polymer homogeneously disperses SWNT in water. Figure 4 contains the picture of the SWNT samples grafted and physically dispersed with PVBTMACl, both subjected to the same ultracentrifugation purification. Both samples contained 0.04 g/L of nanotubes. The sample from the physical mixture fails to disperse since almost all of the polymer was washed out, whereas the grafted sample forms a visually uniform dispersion. The AFM analysis of this sample in Figure 5 shows mostly individual nanotubes and small bundles under 10 nm in diameter. The clumps seem on the micrograph were also observed in AFM of the pristine material. According to the high resolution SEM, (see Figure 4 in Chapter 4) these

particles correspond to aggregates of short nanotubes. The solubility limit of the functionalized SWNT was tested by dissolution of the nanotubes retrieved after centrifugation in different volumes of water. The dispersions were visually homogeneous for the concentrations as high as 0.5 g/L. Above this limit, the dispersions were too dark for observation. The best samples containing 0.1 g/L of the functionalized SWNT in water have been stable for 7 months without precipitation and only a partial aggregation occurred after 2.5 years (November, 2007).

Figure 4. SWNT 0.04 g/L in water, from in-situ polymerization (left) and from physical dispersion with polyelectrolyte (right) after 3 cycles of ultracentrifugation.

The yield of the functionalized material calculated from the gravimetric results was only 50% after low speed centrifugation. This suggests that nanotubes were not functionalized uniformly. The synthetic mixture contained visible aggregates of SWNT so that only outer tubes of the bundles reacted most while the inner tubes were functionalized to a much lower degree. However, the rejected material could be recycled for the next synthesis.

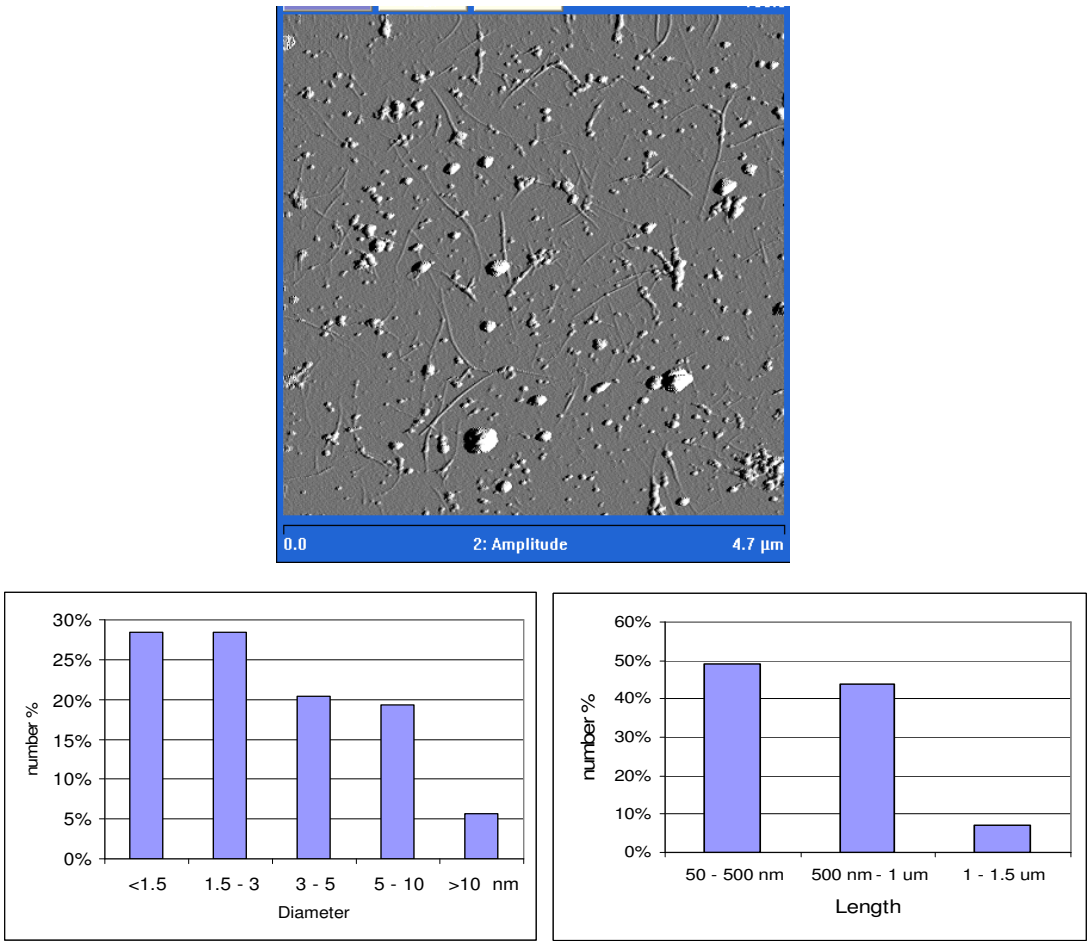

Figure 5. AFM image and size distribution of the SWNT-PVBTMA composite deposited on mica chip.

Layer-by-layer films were created by alternating deposition of SWNT-PVBTMA vs. SWNT-PSS and SWNT-PVBTMA vs. PAA. Figure 6 shows the increase in optical density of the films during the deposition. The previous studies have shown that absorption of the polyelectrolytes in the LBL films is negligible, and an increase in optical density occurs primarily due to the increased nanotube content in the film.[15] The results show that the growth rate of the film built from the oppositely charged nanotubes is slow compared to the SWNT vs. PAA film. The SWNT-PVBTMACl complex

contained 34 % of polyelectrolyte while the SWNT-PSS had only 30 % of PSS, according to TGA. Low surface charge and relative rigidity of nanotubes accounted for the low efficiency of the deposition process in this system. In the SWNT versus PAA system, in contrast, the steady film growth at the reasonable rate, compared to similar experiments reported in literature,[15] was observed. Presumably, PAA provided a flexible cushioning layer for the nanotube layer to sufficiently absorb onto the surface of the film.

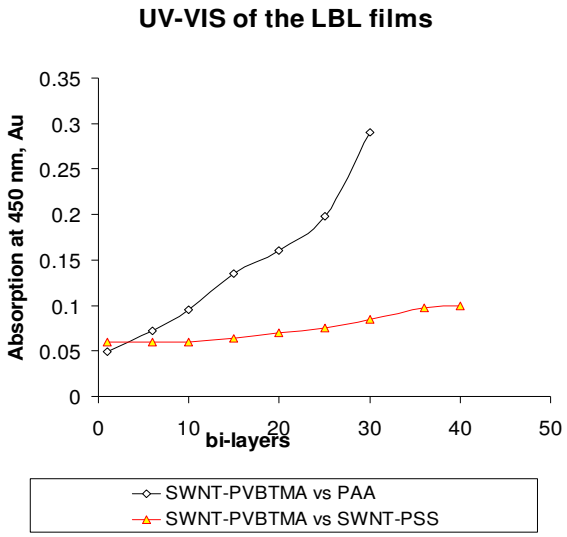

Figure 6. UV-VIS absorption of the growing LBL films.

Conclusions

In-situ polymerization of VBTMA-Cl in the presence of carbon nanotubes resulted in the covalent attachment of the growing polymer chains to nanotubes. The degree of such an attachment is relatively low, which preserves the electronic properties of nanotubes and at the same time allows reasonably good solubility in water at a very low content of the polyelectrolyte. The LBL deposition of this material with PAA has

shown the ability of the SWNT-PVBTMA to form multilayer films which will be especially useful for the processes where low surfactant content, pristine electronic structure, and positive charge of nanotubes are important. This material has been studied at the laboratory of Dirk Guldi, University of Erlangen, Germany, toward interaction with porphyrin and fabrication of photovoltaic coatings, and a manuscript is currently being prepared.[16]

References

(1) Ariga, K. In *Encyclopedia of Nanoscience and Nanotechnology*; Nalwa, H. S., Ed.; American Scientific Publishers: Stevenson Ranch, CA, 2004; Vol. 4, pp 467.

(2) Guldi, D. M.; Rahman, A. Qin, S.; Tchoul, M.; Ford, W. T.; Marcassio, M.; Paolucci, D.; Paolucci, F.; Campidelli, S.; Prato, M. *Chem. Eur. J.* **2006**, *12*, 2152.

(3) Gheith, M. K.; Sinani, V. A.; Wicksted, J. P.; Matts, R. L.; Kotov, N. A. *Adv. Mater.* **2005**, *17*, 2663.

(4) Loh, K. J.; Kim, J.; Lynch, J. P.; Wong Shi Kam, N.; Kotov, N. A. *Smart Mater. Struct.* **2007**, *16*, 429.

(5) Mamedov, A. A.; Kotov, N. A.; Prato, M.; Guldi, D. M.; Wicksted, J. P.; Hirsch, A. *Nature Mater.* **2002**, *1*, 190.

(6) Moore, V. C.; Strano, M. S.; Haroz, E. H.; Hauge, R. H.; Smalley, R. E.; Schmidt, J.; Talmon, Y. *Nano Lett.* **2003**, *3*, 1379.

(7) Matarredona, O.; Rhoads, H.; Li, Z.; Harwell, J. H.; Balzano, L.; Resasco, D. E. *J. Phys. Chem. B* **2003**, *107*, 13357.

(8) Tasis, D.; Tagmatarchis, N.; Georgakilas, V.; Prato, M. *Chem. Eur. J.* **2003**, *9*, 4000.

(9) Bahr, J. L.; Tour, J. M. *J. Mater. Chem.* **2002**, *12*, 1952.

(10) Bahr, J. L.; Tour, J. M. *Chem. Mater.* **2001**, *13*, 3823.

(11) Garg, A.; Sinnott, S. B. *Chem. Phys. Lett.* **1998**, *295*, 273.

(12) Qin, S.; Qin, D.; Ford, W. T.; Herrera, J. E.; Resasco, D. E.; Bachilo, S. M.; Weisman, R. B. *Macromolecules* **2004**, *37*, 3965.

(13) Thomsen, C.; Reich, S. *Phys. Rev. Lett.* **2000**, *85*, 5214.

(14) Dyke, C. A.; Tour, J. M., *J. Phys. Chem. A.*, **2004**, *108*, 11151.

(15) Qin, S.; Qin, D.; Ford, W. T.; Herrera, J. E.; Resasco, D. E. *Macromolecules* **2004**, *37*, 9963.

(16) Rahman, G. M. A.; Sgobba, V.; Troeger, A.; Guldi, D. M. Jux, N.; Tchoul, M. N.; Ford, W. T.; Mateo-Alonso, A.; Prato, M. (manuscript in preparation)

CHAPTER III

GRAFTING OF POLYSTYRENE TO SINGLE-WALLED CARBON NANOTUBES

Abstract

Single-walled carbon nanotubes were covalently grafted with polystyrene via in-situ free radical polymerization. Short time oxidation of nanotubes with diluted nitric acid prior to polymerization increased the yield of functionalized material from 19 % to 35 % due to the splitting of the bundles and increase of the surface area in the SWNT. The resulting materials contained 26–33 % of polystyrene by weight for different samples and had higher solubility in THF and DMF compared to the pristine nanotubes, while the changes in electronic structure were negligible as judged by Raman spectroscopy. Polystyrene composites have been prepared by solution mixing using the functionalized nanotubes.

Introduction

Addition of carbon nanotubes in polymers increases tensile and compressive strength, tensile modulus, glass transition temperature, electrical, and thermal conductivity of the resulting composites.[1,2,3] However, incorporation of carbon nanotubes (CNT) into a polymer matrix is a challenge due to poor miscibility of nanotubes with polymers and the generally low dispersibility of CNT in solvents. There are three classes of techniques for preparation of polymeric composites of CNT: melt blending, solution mixing, and in-situ polymerization.[4] The latter two methods have shown the best results due to a good homogenization of nanotubes and polymer in solution. Dispersion of nanotubes in the solvents is achieved via modification of their surface by either a covalent or a noncovalent approach. Polymeric dispersants have been successfully used for noncovalent functionalization of nanotubes. Poly(4-vinylpyridine) dispersed SWNT in alcohols.[5] PEO-PDMS-PEO[6] copolymer solubilized nanotubes in toluene. Alkyl-substituted poly(phenylene vinylene)[7] and poly(phenylene ethynylene)[8] have been found efficient for obtaining homogeneous dispersions of carbon nanotubes in chloroform. The noncovalent approach is simple and straightforward. However, the main drawback of this method is that the composite will always contain the dispersing agent, which may alter the properties of the polymer.

The covalent approach allows grafting of various compounds to nanotubes, even those that normally don't have a strong adhesion to them. In the experiments of Dyke and Tour,[9] addition of 49% by weight of 4-chlorophenyl groups to SWNT via diazonium chemistry increased solubility of the functionalized nanotubes in organic solvents by an order of magnitude. Covalent grafting of various moieties to nanotubes has been achieved

also via nitrene addition,[10] azomethyne ylide addition,[11] and addition of polymer radicals during in-situ polymerization,[12] as well as via esterification and amidation of the carboxylic groups on oxidized nanotubes.[13] In all of these reactions, efficient solubility of nanotubes in organic solvents was achieved. As discussed above, the principal problem of the covalent functionalization is distortion of electronic structure of carbon nanotubes.

The advantages of non-covalent and covalent functionalization can be combined by grafting polymers to carbon nanotubes. Long chains attached to nanotubes can keep them dispersed due to a steric repulsion,[6] for which a small number of chains on the surface is needed. As a result, the polymer-functionalized nanotubes demonstrate high solubility in solvents with a low degree of functionalization.[13] For example, in the experiments of Qin, the molecules of polystyrene grown from the surface of SWNT by ATRP polymerization allowed stable dispersions of the functionalized material in DMF and THF, while only 1 polymer chain per 240 carbon atoms was attached.[14]

If the polymer-functionalized carbon nanotubes are to be used in polymeric composites, it is very important that the attached polymer is miscible with the host polymer. In the most cases, different polymers are poorly miscible with each other,[15] so the attached polymer even though providing a high solubility for nanotubes, might force such into a separate fraction as the solvent evaporates during the composite preparation. The objective of this work was to study the incorporation of the polymer-functionalized carbon nanotubes in polystyrene, so the best choice for the polymer to graft to nanotubes is polystyrene too. Grafting by in-situ free radical polymerization is a simple and potentially scalable process which was successfully applied in the past for grafting

poly(sodium 4-styrenesulfonate),[16] poly(4-vinylpyridine)[12] and poly(vinylbenzyl trimethylammonium chloride) to SWNT.

Experimental

Materials. Purified HiPco™ single-walled carbon nanotubes, batch #P0340, were purchased from Carbon Nanotechnologies Inc., Houston, TX. TGA analysis in air found 15 % residue at 800 °C, which accounts for 10% of iron catalyst in the material. Styrene was obtained from Acros Organics and purified by passing through basic alumina. AIBN (2,2'-azobisisobutyronitrile) was obtained from Aldrich and purified by recrystallization from methanol. N,N-Dimethylformamide (DMF) was obtained from Pharmco and dried over anhydrous potassium carbonate. All other chemicals were purchased from Aldrich and used as received.

Instruments and measurements. Ultrasonication was performed using a Fisher FS-30 160W 3QT ultrasonic cleaner or a Microson XL-2000 22 KHz ultrasonic cell disruptor. The solutions were filtered under vacuum using a glass cell and 0.45 μm porous PTFE membranes. Raman spectra in the range of 1200–1800 cm^{-1} were acquired in backscattering geometry using a Jobin-Yvon U1000 double grating spectrometer and an Argon ion laser, 514.5 nm (2.41 eV), at an intensity of 16.2 kW/cm^2, focused through a 0.80 NA objective (Olympus). The scattered light was analyzed using an electronically cooled photomultiplier tube (Hamamatsu 943-02). Data were taken with a 0.5 cm^{-1} step size and 1.5 s integration time in photon counting mode. The samples were prepared by applying a suspension on a clean silicon surface followed by drying at 100 °C to yield a solid surface coating. Atomic force micrographs were obtained using a Multimode

Nanoscope IIIa SPM (Digital Instruments, Santa Barbara, CA) operating in the tapping mode. The samples were prepared by applying a drop of a DMF or THF suspension on a mica chip (10 min for DMF and 1 min for THF), followed by removing the liquid and drying the substrate in the nitrogen flow. To estimate the size distribution, lengths and heights of at least 100 tubular objects from 2 or more images taken from different spots of the substrate were measured. Thermogravimetric analyses were performed using a Shimadzu TGA50/50H instrument in nitrogen. The optical microscopy of the films was performed on a Leica DM IRB optical microscope at 100x magnification. The UV-VIS spectra were obtained on a Cary-5000 UV-VIS-NIR spectrometer in the wavelength range of 200–2000 nm. Scanning electron microscopy was performed on a JEOL JSM 6400 Scanning Electron Microscope operating at 27 kV accelerating voltage.

In-situ functionalization of SWNT with polystyrene. For this experiment both pristine ($SWNT_P$) and oxidized ($SWNT_O$) nanotubes were used. The outline of the experiments is presented in Scheme 1. Oxidation of SWNT was performed according to the previously reported procedure, by bath sonication in 8 M HNO_3 for 60 min followed by washing out the acid and redispersion of the solid in DMF by bath sonication.[17] Either $SWNT_P$ or $SWNT_O$ in the amount of 50 mg were dispersed in 50 mL of DMF by bath sonication for 60 min, followed by stirring for 12 h and tip-sonication for 15 min at 5 W immediately prior to synthesis. The dispersion was mixed with 6.5 g of styrene and 100 mg of AIBN (molar ratio of [styrene]:[AIBN]:[SWNT carbon] ≈ 100:1:6.5) and transferred to a 100-mL Schlenk flask equipped with a stirring bar. The flask was degassed by 3 freeze-pump-thaw cycles. Degassing is a crucial step and has to be done thoroughly. Oxygen in the system greatly reduces the yield of the functionalized nanotubes. The flask was immersed

in a thermostated oil bath at 75 °C under stirring. After 48 h, the mixture was cooled to room temperature, vacuum-filtered through a 0.45 µm PTFE membrane and washed on the filter with 30 mL of chloroform to remove the free polystyrene. The washing was repeated several times until the addition of 5 drops of filtrate to 10 mL of methanol resulted in no cloudiness, indicating that little or no soluble polystyrene remained, giving the samples $SWNT_P$-PS and $SWNT_O$-PS (Scheme 1). During the washing, the solid was covered with the solvent at all times and was never allowed to dry, since the dry mat of SWNT is extremely difficult to disperse homogeneously in solvents. The solid from the filter was dispersed in 500 mL of THF by bath sonication for 1 h, followed by centrifugation at 5000g for 1 h. The supernatant was decanted. The precipitate was subjected to one more cycle of dispersion-centrifugation. The supernatants from the two cycles were combined, vacuum-filtered through the 0.45 µm PTFE membrane, and the solid was dried at 100 °C until constant mass, giving the samples $SWNT_P$-PS-sup and $SWNT_O$-PS-sup respectively. The outline of the experiments is presented in Scheme 1.

Scheme 1. Experimental procedure

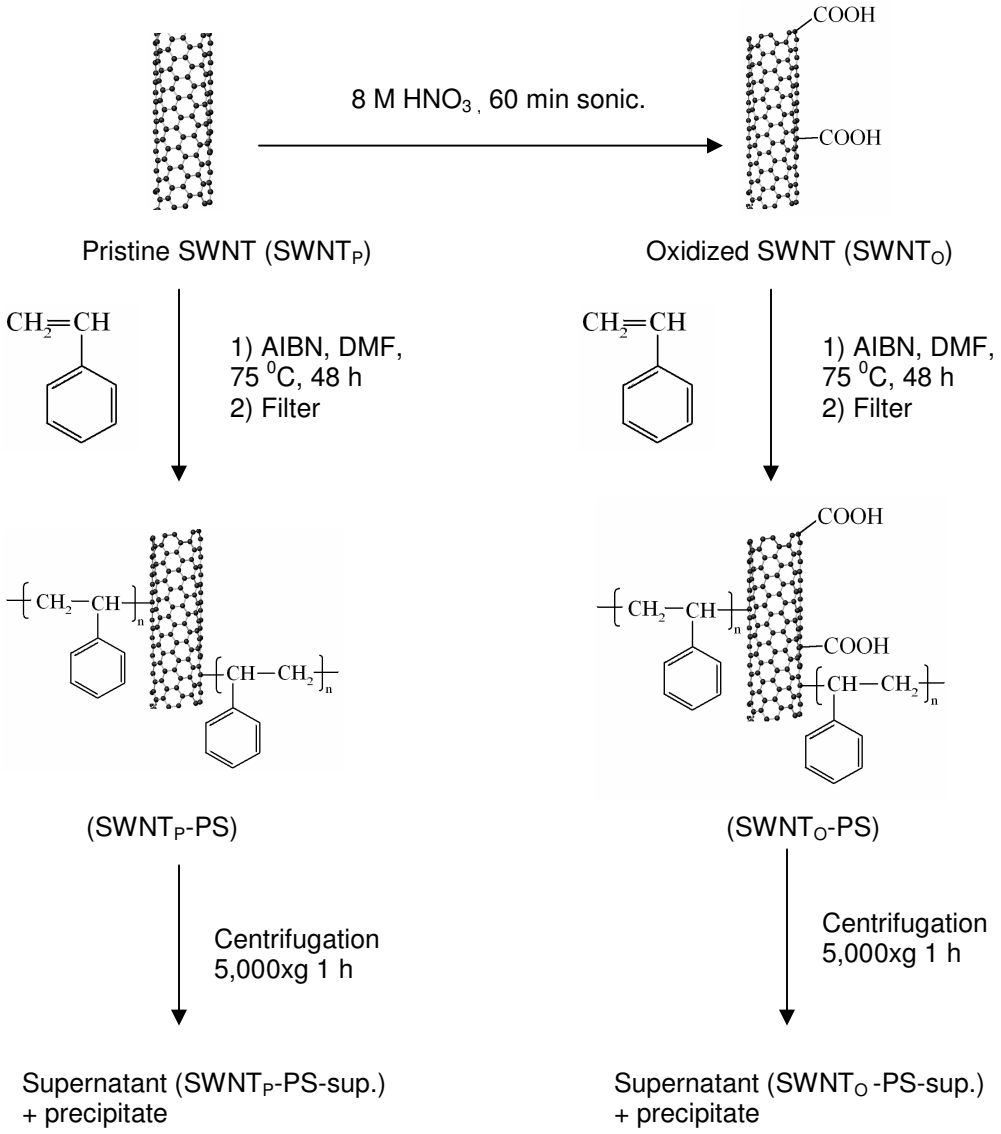

Mixing SWNT with a separately synthesized polystyrene (control experiment). In order to evaluate the ability of polystyrene to disperse carbon nanotubes, the samples of both pristine and oxidized HiPco SWNT were mixed with a sample of polystyrene that was synthesized separately. For the synthesis, 8.7 g of styrene and 138 mg of AIBN (molar ratio of [styrene]:[AIBN] = 100:1) were dissolved in 60 mL of DMF in a 100-mL

Schlenk flask equipped with a stir bar, the mixture was degassed by 3 freeze-pump-thaw cycles, and polymerization was carried out in an oil bath at 75 °C under stirring for 24 h. The solid was isolated by precipitation in 300 mL of methanol, filtering and drying in vacuum to a constant mass of 4.6 g. The SEC molecular weights were M_N = 9600 and M_W/M_N = 1.7. A 40 mL sample of 0.5 g/L DMF dispersion of SWNT was mixed with 2 g of the synthesized polystyrene by 30 min bath sonication, followed by stirring at 75 °C for 48 hours. The mixture was filtered and washed with chloroform according to the procedure described above. The solid was redispersed in 200 mL of THF by 60 min of bath sonication, followed by centrifugation at 5000g for 60 min. All nanotubes precipitated during centrifugation of both pristine and oxidized samples.

Composites of functionalized SWNT and polystyrene. $SWNT_O$-PS in the form of the 0.5 g/L dispersion in DMF was used for composites. Typically 5–50 mL of this dispersion was diluted with DMF by 1:10 and bath sonicated for 60 min. The 20 g/L solution of polystyrene in DMF was prepared separately. The dispersion of SWNT was mixed with the solution of polystyrene in a ratio yielding the required proportion of nanotubes and polystyrene. The mixture was stirred for 1 h, followed by bath sonication for 30 min. The resulting mixture was precipitated by pouring into a 10-fold volume of water vigorously mixed with a mechanical stirrer followed by filtration, washing the solid with water and methanol and drying at 110 °C for 1 h.

Samples for electrical conductivity measurements were pressed into 15x15x0.5 mm pieces using a heat press and a custom made picture frame mold. The sample in the mold was heated up to 175 °C followed by applying the 10,000 psi pressure for 1 min, releasing the pressure, taking the mold out of the press, and cooling it on the bench. Thin

films (50 ± 10 μm) of the composites for microscopy and spectroscopy were pressed by sandwiching between two steel plates using the same press and conditions.

Results and Discussion

In-situ polymerization of styrene in the presence of SWNT was expected to attach polystyrene chains to the carbon atoms on the surface of nanotubes. The mild nitric acid oxidation of nanotubes significantly increased the solubility of the resulting material in DMF and decreased the diameter of bundles,[17] thus providing the larger surface area for the reaction with polymer radicals. We used the oxidized nanotubes for the synthesis in anticipation that the expanded surface area would increase the degree of functionalization of this material.

Figure 1 contains the Raman spectroscopy results for the different SWNT materials. As in the previous chapter, the intensity of the D-band (I_D) at 1320 cm^{-1} (arising due to sp^3 defects in the structure of the nanotube sidewall) with respect to the intensity of the G-band (I_G) 1590 cm^{-1} (corresponding to the longitudinal stretching vibrations of the sp^2 carbons) was used to confirm the covalent attachment of polystyrene to nanotubes. The results are presented in Table 1.

Figure 2 shows the AFM micrographs of pristine and oxidized SWNT before and after the synthesis. Length and diameter distribution within bundles in different samples is presented in Figure 3, and results for the average length and diameter are included in Table 1.

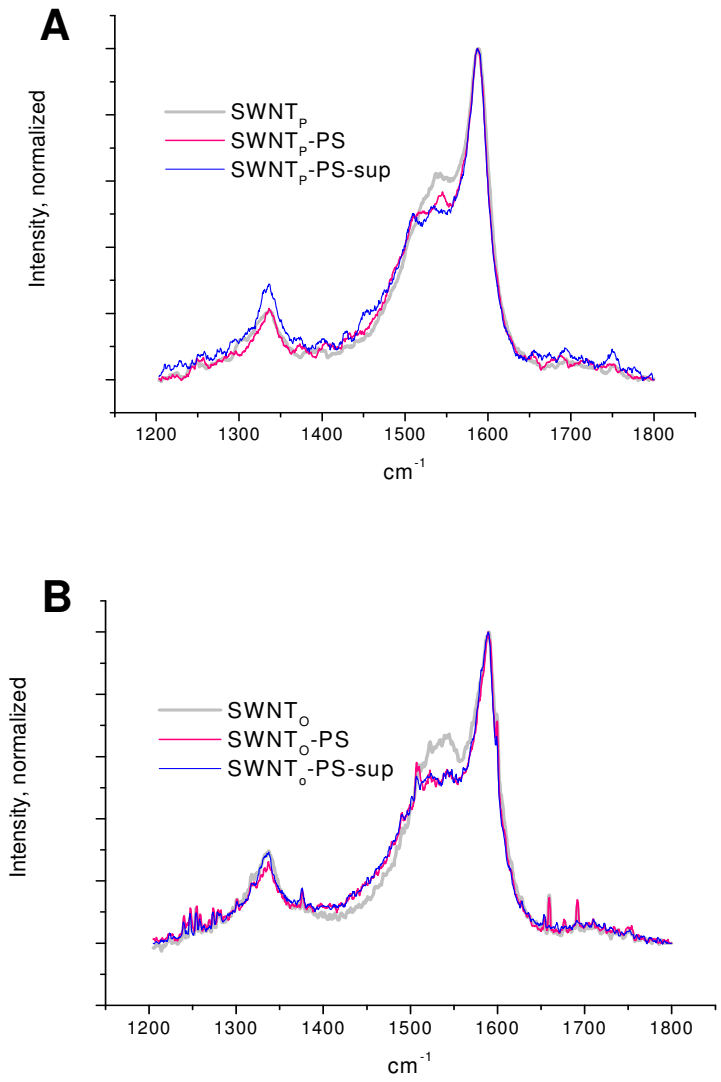

Figure 1. Raman spectra using 514.5 nm excitation of the pristine (A) and oxidized (B) SWNT before and after in-situ polymerization.

It was difficult to deposit sufficient amount of pristine and functionalized pristine nanotubes on the hydrophilic mica chips, presumably due to a high hydrophobicity of these materials. In order to have at least 100 objects for statistics, 6 images from the different spots of the substrates were used. The oxidized and functionalized oxidized

nanotubes, in contrast, deposited easily, providing a large number of objects for the measurements. The polystyrene functionalized oxidized SWNT were found to assemble into long fibrous structure during deposition from dispersion onto mica, as seen in Figure 2D. Presumably, the presence of both hydrophilic and hydrophobic moieties on the surface of these nanotubes was responsible for such an assembly.

Table 1. Characterization of the SWNT materials

Sample	TGA and gravimetry		AFM		Raman
	SWNT*, mg	SWNT:PS**, %	<L>, nm	<d>, nm	I_D:I_G***
$SWNT_P$	50.0	-	890	8.0	0.20±0.05
$SWNT_P$-PS	50.0	73:27	700	4.9	0.20±0.05
$SWNT_P$-PS-sup	9.5	68:32	550	4.2	0.30±0.05
$SWNT_O$	50.0	-	690	6.1	0.28±0.05
$SWNT_O$-PS	50.0	74:26	820	7.5	0.25±0.05
$SWNT_O$-PS-sup	17.5	67:33	730	7.7	0.29±0.05

*Weight of SWNT in the sample, by gravimetry and TGA
**Weight fractions of SWNT and PS in the sample, by TGA
***Average for 3 spectra acquired from different spots of the sample was calculated

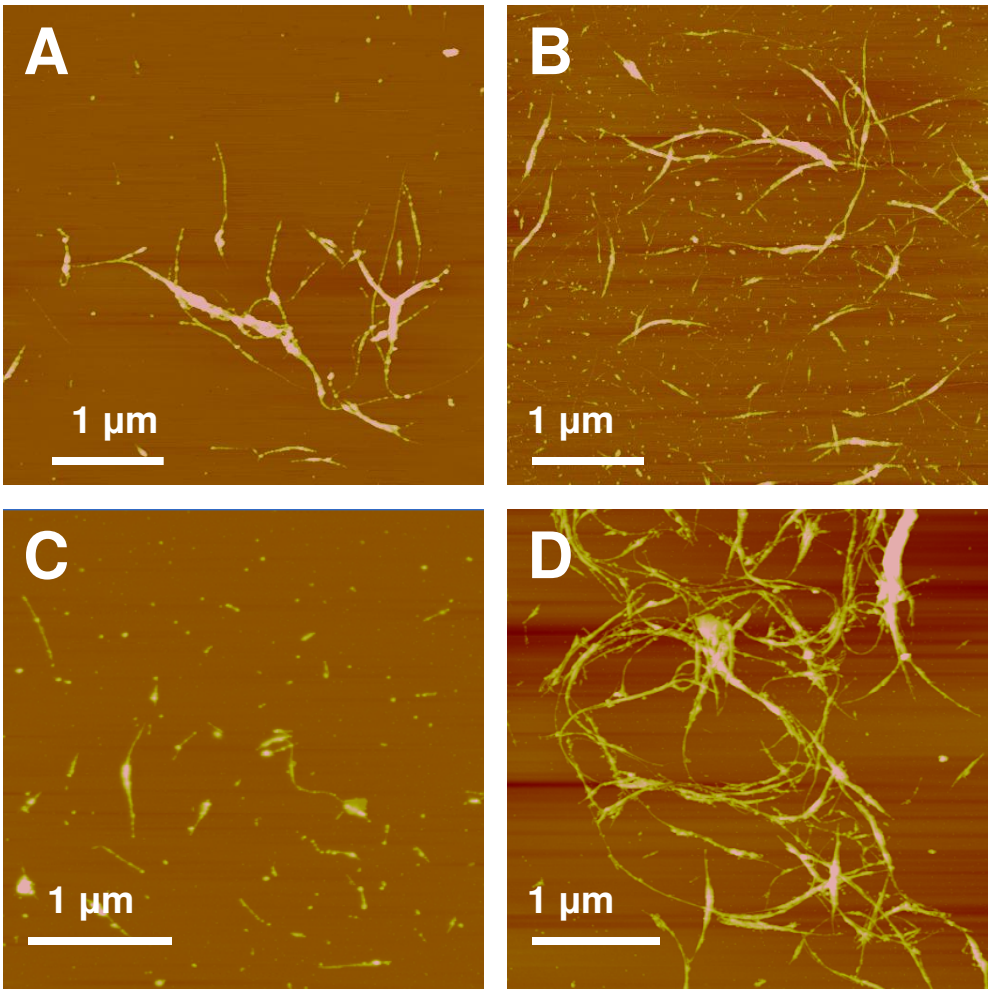

Figure 2. AFM of the SWNT samples: pristine (A), oxidized (B), pristine after in-situ polymerization (C) and oxidized after the in-situ polymerization (D).

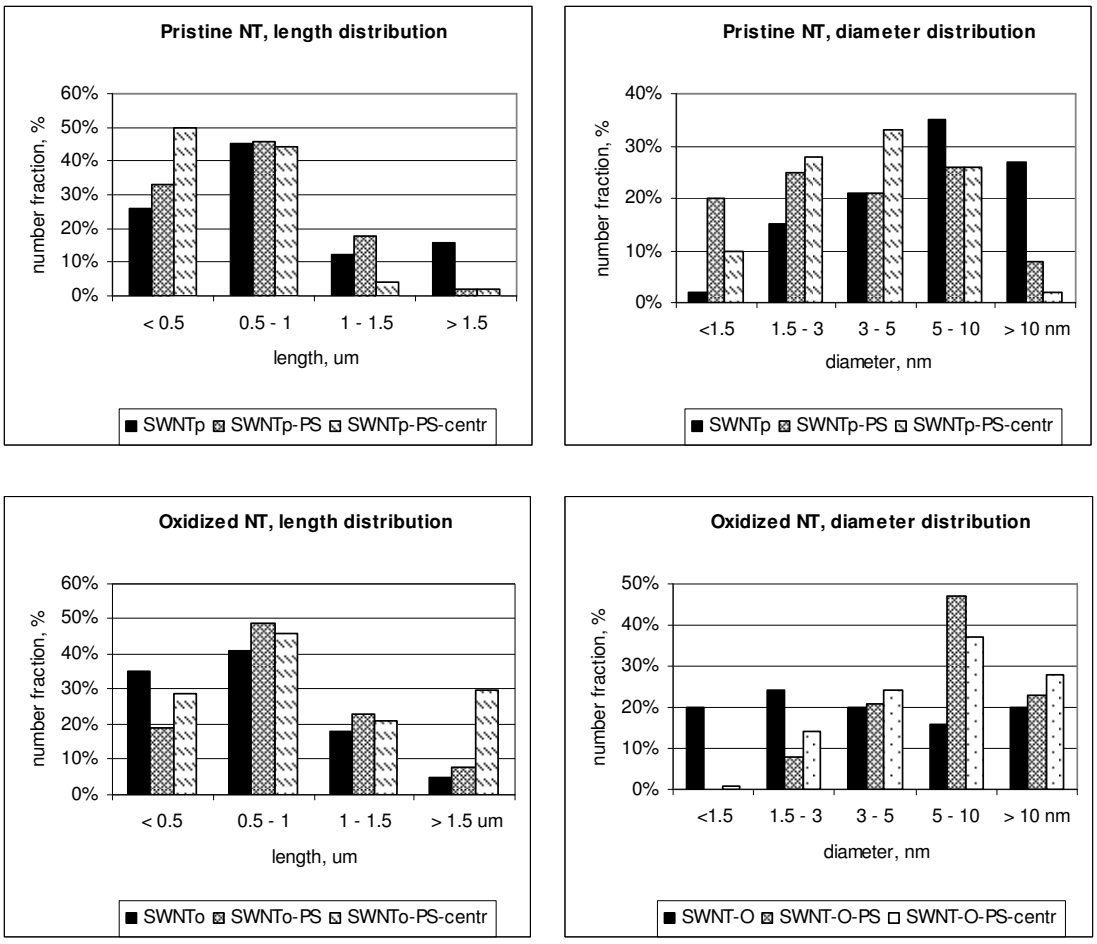

Figure 3. Size distribution within nanotube bundles in the samples.

According to the Raman spectral data, there was no change in I_D/I_G after the synthesis with pristine nanotubes, but the supernatant after centrifugation showed a 50% increase in this parameter. The nanotubes in dry pristine material are entangled and bundled, resulting in the presence of large aggregates in the reaction mixture. The tubes on the outside of the bundles are exposed to the reagent whereas the inner tubes are hindered and may react to a lesser degree. Sonication breaks the bundles and centrifugation should precipitate the less functionalized fraction of the sample, leaving the more functionalized part in solution. According to TGA results (Table 1), the samples

$SWNT_P$-PS-sup and $SWNT_O$-PS-sup contained more polystyrene which suggests that nanotubes in these materials had a higher degree of functionalization.

There was a problem using Raman spectroscopy to detect covalent functionalization in the experiment with the oxidized SWNT sample. Small deviations in the I_D/I_G ratio do not provide for a confident evidence of such functionalization. The best evidence of the covalent functionalization is the solubility of the resulting material $SWNT_O$-PS in THF (0.05 g/L), while oxidized nanotubes $SWNT_O$ could not be dispersed in this solvent with addition of the separately synthesized polystyrene in the control experiment.

The oxidized SNWT, after the PS grafting, were more soluble in THF than the pristine SWNT grafted with PS so that 17.5 mg of $SWNT_O$-PS-sup was separated by centrifugation, giving a yield of 35 %. The first supernatant contained 11.0 mg of the SWNT, corresponding to the concentration of 22 mg/L in THF. The sample of this solution has been stable for 2 months to date without precipitation. Functionalization of pristine nanotubes resulted in only 9.5 mg of $SWNT_P$-PS-sup separated by centrifugation, giving a yield of 19 %. Mild nitric acid oxidation is known to effectively break up the aggregates and decrease the diameter of bundles,[17] as it will be shown in Chapter 4, thus providing a higher surface area of the SWNT for reaction with polystyrene radicals. Since the absolute value of the I_D/I_G of the supernatant fractions was the same in both experiments, we can assume that the degree of functionalization was approximately equal. However, the smaller bundles and higher surface area in the oxidized sample made it possible to functionalize more nanotubes.

Covalent functionalization was expected to exfoliate bundles of nanotubes, decreasing their diameter, as reported in literature.[16,18] This effect was indeed observed in

the reaction of pristine nanotubes. The average diameter of bundles in the samples $SWNT_P$-PS and $SWNT_P$-PS-sup was 4.9 nm and 4.2 nm, respectively, in contrast to 8.0 nm for the pristine sample. In the case of oxidized SWNT, on the contrary, SWNT bundles after functionalization became even larger, 7.5 nm for $SWNT_O$-PS and 7.7 nm for $SWNT_O$-PS-sup, in contrast to 6.1 nm for the starting material. We can exclude contribution of the layer of attached polystyrene to the increased bundle diameter in these two samples, since the polymer content was nearly the same in all functionalized samples. The lengths of the bundles in the functionalized oxidized nanotubes $SWNT_O$-PS and $SWNT_O$-PS-sup increased as well in respect to the starting sample $SWNT_O$, mostly due to a larger fraction of objects with the length of 1.5 μm or more. Figure 4 shows long yarns of the nanotubes in the $SWNT_O$-PS sample that at closer examination appeared to be shorter bundles connected by the ends. The surface of these nanotubes has both hydrophilic carboxylic groups[19] and hydrophobic polystyrene molecules. The surface of mica is highly hydrophilic. A much larger number of tubes on the surface was observed for the functionalized oxidized nanotubes (Figures 2D and 4) compared to the functionalized pristine nanotubes (Figure 2C), suggesting that surface of the bundles of $SWNT_O$-PS and $SWNT_O$-PS-sup should be hydrophilic as well. We assume that during the deposition on mica the core-shell structure of bundles with polystyrene chains inside and oxidized SWNT surface outside may be formed, accounting for the larger bundles in these materials.

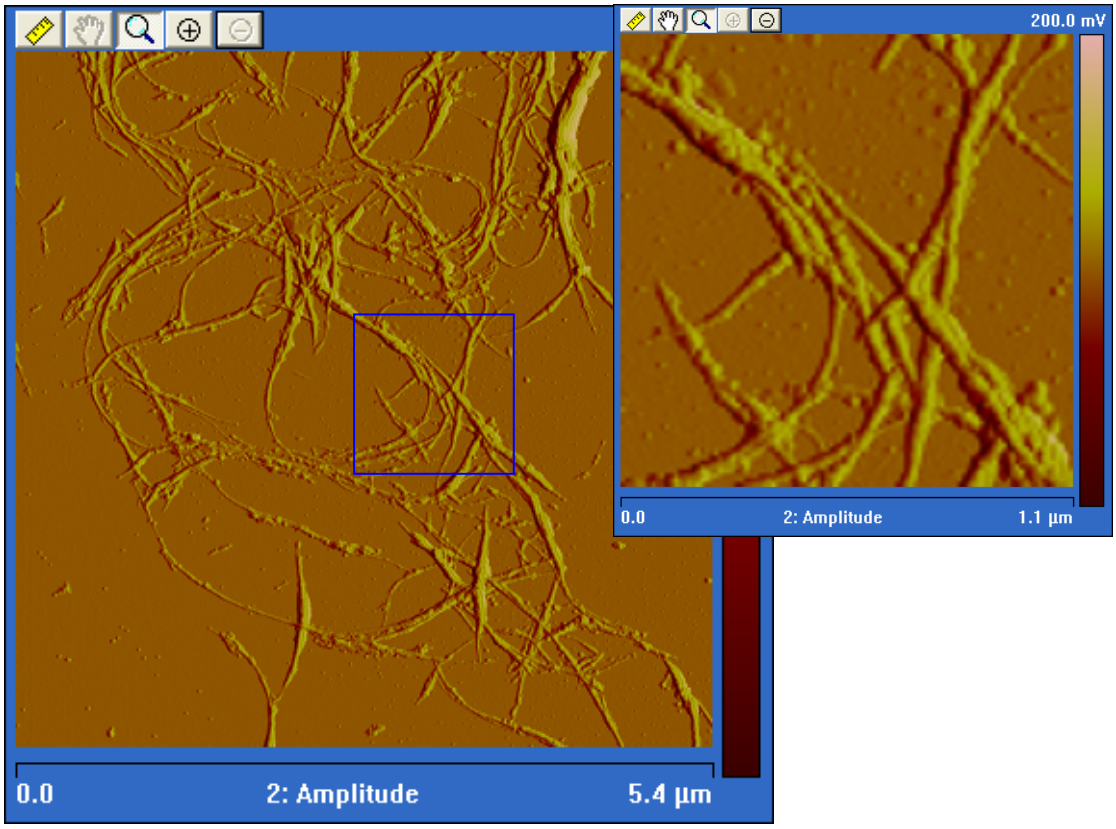

Figure 4. AFM of the $SWNT_O$-PS sample on Mica chip. The close-up image shows the connection between different bundles.

The sample $SWNT_O$-PS was used for the preparation of composites with polystyrene because of the higher yield of the functionalized nanotubes in this sample. Stable uniform dispersions in DMF at concentration as high as 100 mg/L can be obtained, whereas for oxidized nanotubes before functionalization only a 30 mg/L concentration could be achieved. Figure 5 shows the SEM images of the composite containing 1.3 % SWNT in polystyrene. Image A was taken from the surface that was sputter-coated with Au/Pd and shows only morphology of the surface. Images B and C were taken on the same spot of the sample before it was coated and reveal the uniformly distributed bundles. This technique allows imaging nanotubes located up to 50 nm beneath the

surface.[20] The concentration of nanotubes has to be above the percolation threshold in order to effectively dissipate electrons in the SEM. Electrical properties of the composites will be discussed in Chapter 5 of this work.

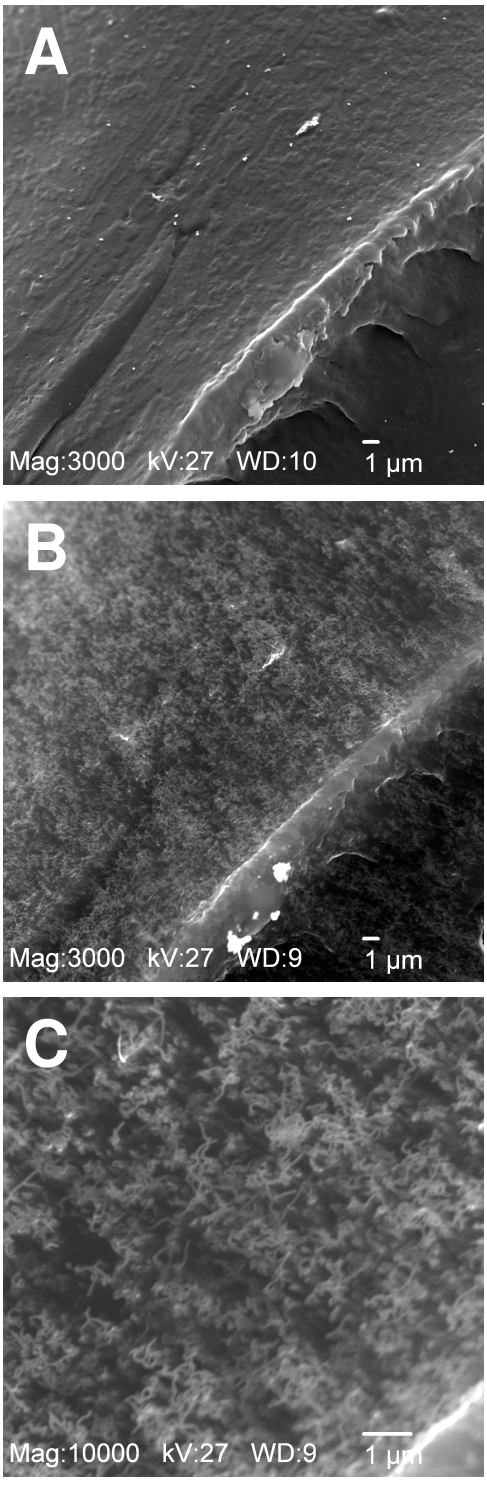

Figure 5. Scanning electron microscopy of the 1.3 % SWNT composite in polystyrene. A – coated with Au/Pd surface; B, C – uncoated surface.

Conclusions

Attachment of a very low amount of polystyrene to carbon nanotubes can make a noticeable difference in their solubility in organic solvents. Dispersion state of nanotubes in the reaction is critical for the efficiency of the functionalization. Since nanotubes do not ideally dissolve in any of the solvents but rather form colloidal dispersions of bundles of different size, the functionalization is dependent on the accessibility of the SWNT surface to the reagent during the reaction. Therefore, the greater the nanotubes are dispersed initially, the more efficiently they will react. Better dispersion of oxidized nanotubes in DMF resulted in a higher yield of the functionalized material. Interestingly, the degree of covalent attachment was not higher for this sample. In other words, more polystyrene did not attach to nanotubes, but polystyrene attached to more nanotubes.

References

(1) Coleman, J. N.; Khan, U.; B.; Blau, W. J.; Grin'ko, Y. K. *Carbon* **2006**, *44*, 1624.

(2) Winey, K. I.; Kashiwagi, T.; Mu, M. *MRS Bulletin* **2007**, *32*, 348.

(3) O'Connell, M. J., Ed. *Carbon Nanotubes: Properties and Applications*; CRC Press: Boca Raton, FL, 2006.

(4) Moniruzzaman, M.; Winey, K. I. *Macromolecules* **2006**, *39*, 5194.

(5) Rouse, J. H. *Langmuir* **2005**, *21*, 1055.

(6) Shvartzman-Cohen, R.; Levi-Kalisman, Y.; Nativ-Roth, E.; Yerushalmi-Rozen, R. *Langmuir* **2004**, *20*, 6085.

(7) Star, A. J.; Stoddart, F.; Steuerman, D.; Diehl, M.; Boukai, A.; Wong, E. W.; Yang, X.; Chung, S.-W.; Choi, H.; Heath, J. R. *Angew. Chem. Int. Ed.* **2001**, *40*, 1721.

(8) Chen, J.; Liu, H.; Weimer, W. A.; Halls, M. D.; Waldeck, D. H; Walker, G. C. *J. Am. Chem. Soc.* **2002**, *124*, 9034.

(9) Dyke, C. A.; Tour, J. M. *Chem. Eur. J.* **2004**, *10*, 812.

(10) Holzinger, M.; Abraham, J.; Whelan, P.; Graupner, R.; Ley, L.; Hennrich, F.; Kappes, M.; Hirsch, A. *J. Amer. Chem. Soc.* **2003**, *125*, 8566.

(11) Georgakilas, V.; Kordatos, K.; Prato, M.; Guldi, D. M.; Holzinger, M.; Hirsch, A. *J. Am. Chem. Soc.* **2002**, *124*, 760.

(12) Qin, S.; Qin, D.; Ford, W. T.; Herrera, J. E.; Resasco, D. E. *Macromolecules* **2004**, *37*, 9963.

(13) Lin, Y.; Meziani, M. J.; Sun, Y.-P. *J. Mater. Chem.* **2007**, *17*, 1143.

(14) Qin, S.; Qin, D.; Ford, W. T.; Resasco, D. E.; Herrera, J. E. *Macromolecules* **2004**, *37*, 752.

(15) Hope, M. J. Folkes, P. S., Ed. *Polymer Blends and Alloys*; Chapman & Hall: London, UK, 1993.

(16) Qin, S.; Qin, D.; Ford, W. T.; Herrera, J. E.; Resasco, D. E.; Bachilo, S. M.; Weisman, R. B. *Macromolecules* **2004**, *37*, 3965.

(17) Tchoul, M. N., Ford, W. T.; Lolli, G.; Resasco, D. E.; Arepalli, S. *Chem. Mater.* **2007**, *19*, 5765.

(18) Dyke, C. A.; Tour, J. M. *Nano Lett.* **2003**, *3*, 1215.

(19) Zhang, J.; Zou, H.; Qing, Q.; Yang, Y.; Li, Q.; Liu, Z.; Guo, X.; Du, Z. *J. Phys. Chem. B* **2003**, *107*, 3712.

(20) Loos, J.; Alexeev, A.; Grossiord, N.; Koningc, C. E.; Regev, O. *Ultramicroscopy* **2005**, *104*, 160.

CHAPTER IV

OXIDATION OF SINGLE-WALLED CARBON NANOTUBES WITH NITRIC ACID

Abstract

Oxidation of single-walled carbon nanotubes with nitric acid increases their dispersability in water, methanol, and N,N-dimethylformamide (DMF). Two oxidation protocols, sonication in 8 M HNO_3 at 40 °C and reflux in 2.6 M HNO_3, have been examined. SWNT produced by CoMoCat™, HiPco™ and Pulsed Laser Vaporization (PLV) methods have been evaluated. A noticeable increase in dispersability occurred already after one hour of sonication for all types of nanotubes and 2–4 hours of reflux for different types of nanotubes. Longer treatments resulted in little further improvement in solubility. Stable uniform dispersions in DMF of CoMoCat SWNT at concentrations as high as 0.4 g/L have been achieved without the use of surfactants or additional chemical functionalization. Raman spectroscopy showed covalent functionalization of the SWNT, which effect was higher for the reflux procedure. At the same time oxidation resulted in shortening of nanotubes and an overall loss of material. The effect of oxidation on properties of nanotubes depended on the type of material. The shortening and functionalization was the highest for CoMoCat SWNT and the lowest for PLV SWNT due to a difference in nanotube diameter. The reflux procedure was found to be more destructive to nanotubes than the sonication procedure.

Introduction

Oxidation of carbon nanotubes has become a basic technique for their chemical modification.[1] Carboxylic groups created on the CNT surface as a result of oxidation[2-4] provide opportunity to attach different molecules of interest[5-8] or seed precursors for the "grafting-from" polymerization.[6,9,10] Chemically modified carbon nanotubes can be further dissolved in different solvents[5,11-13] or incorporated into a polymer matrix.[7,14,15] When we first observed the increased dispersability of nanotubes oxidized with nitric acid in some polar solvents, we directed the effort to a study of this effect with the aim of utilizing the oxidized nanotubes in preparation of polymeric composites by solution processing without further chemical modification. Oxidation is known to damage nanotubes resulting in structural defects,[4] shortening of tubes,[16] accumulation of carbonaceous impurities,[17] disappearance of small diameter nanotubes,[18-20] and an overall loss of material.[17,21] Therefore the objective of this project was to find the oxidation procedure allowing a higher dispersability of nanotubes with minimal structural damage.

According to the literature, nitric acid has been the most frequently utilized agent for oxidation of carbon nanotubes. Various techniques involving HNO_3 can be resolved into two basic approaches: (1) treatment with boiling diluted (2 to 3 M) nitric acid for 16 to 48 hours,[2,4,16,22] and (2) treatment with a mixture of concentrated nitric and sulfuric acids (usually 1:3 by volume) in an ultrasonic bath for 3 to 5 hours.[2,4,7,8,23]

Procedures employing piranha solution (96% H_2SO_4, 30% H_2O_2 by volume),[24] ozone,[25] H_2O_2,[20] and $KMnO_4$[4] have been reported also, but they have not been used as frequently as the nitric acid procedures.

Treatment of nanotubes with dilute nitric acid was first introduced by A. Rinzler,[16] primarily as a purification procedure for the material produced by laser vaporization. Nanotubes were refluxed in 2.6 M HNO_3 for 45 hours. Such a treatment reduced metal content and improved separation of amorphous carbon from nanotubes during the next step of cross-flow filtration. This procedure, being less destructive than the concentrated acid treatment, was adopted by many other researchers with some modifications in temperature and time.[9,17,26-28] However, the effect of diluted nitric acid on different SWNT material has not been sufficiently studied.

Treatment with the mixture of concentrated sulfuric and nitric acids, as well as the treatment with piranha solution (mixture of sulfuric acid and hydrogen peroxide), were first introduced by Liu[2] as the methods for shortening of nanotubes. The shortening rate of the PLV SWNT was estimated to be 130 nm/hour for H_2SO_4/HNO_3 and 200 nm/hour for piranha during a bath sonication. Both of these solutions as well as single concentrated H_2SO_4, HNO_3 or H_2O_2, were found to selectively eliminate smaller diameter nanotubes from the material.[18-20] Concentrated acids have shown a specific selectivity toward small metallic tubes[19] whereas hydrogen peroxide destroyed preferentially small semiconducting nanotubes.[20]

Owing to carboxylic acid groups, oxidation should make carbon nanotubes more soluble in polar solvents. Although partial solubility of SWNT in water after oxidation has been mentioned in the literature,[23,26,29] to our knowledge, the effect of oxidation on solubility has not been studied in detail. Here we report the increase in solubility of nanotubes in DMF, water and methanol after a short time of oxidation by a dilute nitric acid. The treatment allows dissolving nanotubes without dispersing agents, which can

simplify the preparation of nanotube-based composites and coatings. We also show that carboxylation of the nanotube surface during acid treatment is always accompanied by cutting and etching of the nanotubes. The experimental results presented in this Chapter can assist researches in finding a balance between increasing useful effect and destroying the nanotubes.

Experimental

Materials. Single-walled carbon nanotubes produced by CoMoCat,[30] HiPco[31] and pulsed laser vaporization (PLV)[32] processes were used in this work. CoMoCat nanotubes in the form of a 2% aqueous gel, grade S-P94-02gel, batch # OSU-A-007, purified by the basic (alkali) protocol[33] were obtained from Southwest Nanotechnologies, Inc., Norman, OK. As-produced HiPco material in the form of a puffy fibrous powder, lot # R0488, was obtained from Carbon Nanotechnologies, Inc., Houston, TX. Laser Oven SWNT in the form of a black powder, batches ## JSC-334, 335 and 338, purified by the soft-baking protocol,[34] were obtained from NASA Johnson Space Center, Houston, TX. All the solvents were obtained from Pharmco and Spectrum and dried over anhydrous potassium carbonate. All other chemicals were obtained from Sigma and Aldrich.

Instruments and measurements. Ultrasonication was performed using a Fisher FS-30 160W 3QT ultrasonic cleaner or a Microson XL-2000 22 KHz ultrasonic cell disruptor. Centrifugation was performed on an IEC EXD centrifuge (IEC, Needham, MA). UV-VIS absorption in the range of 400–1100 nm was analyzed using a HP8453 spectrophotometer (Hewlett Packard) and glass cells. Filtration of the solutions was done using a vacuum glass filtration cell and 0.45μm porous PTFE membranes. Atomic force

micrographs were obtained using a Multimode Nanoscope IIIa SPM (Digital Instruments, Santa Barbara, CA) operating in the tapping mode. The samples were prepared by applying a drop of a suspension on a mica chip for 10 min, followed by removing the excess liquid and drying the chip in the nitrogen flow. For the size distribution, lengths and heights of 100 or more objects from 2 or 3 different spots of the substrate were measured. Raman measurements were carried out using a Coherent He-Ne laser operating at an excitation wavelength of 633 nm. The laser power varied from 0.89 to 3.0 mW for different samples; the time for a scan was 60 s. The solid samples were prepared by filtering the DMF solutions using 0.2 μm PTFE membranes. The back-scattered light was analyzed using a Jobin Yvon LabRam 600 single grating spectrometer with a CCD detector. Thermogravimetric analysis was performed on a Shimadzu TGA50/50H instrument. Samples were analyzed in the range of 20–800 °C in air flow at the scan rate of 5 °/min.

Oxidation of carbon nanotubes by 8 M nitric acid with sonication. For this experiment all SWNT materials were first dispersed in DMF at concentration of 0.5 g/L by bath sonication for 40 min at 40–50 °C. In a typical procedure, 20 mL of the 0.5 g/L DMF dispersion of SWNT was filtered, and washed on the filter with 10 mL of methanol and 10 mL of water. The solid was transferred into 20 mL of 8 M HNO_3 in a glass vial, and the mixture was bath sonicated at 40–50 °C for a time ranging from 30 min to 5 hours. The mixture was diluted 1:2 with deionized water and filtered using a 0.45 μm PTFE filter. The solid was washed on the filter with water until the filtrate was neutral, washed with 10 mL of methanol and 10 mL of DMF and redispersed in 20 mL of DMF by bath sonication for 60 min. The filtrates from CoMoCat and HiPco nanotubes were

colorless, but the filtrate from PLV nanotubes was gray. AFM analysis of the filtrate has indicated presence of nanotubes.

Oxidation of carbon nanotubes by 2.6 M nitric acid at reflux. For this experiment all SWNT materials were used as received. In a typical procedure, 20 mg of the material was transferred into a round bottom flask filled with 40 mL of 2.6 M HNO_3 and equipped with a stir bar and a reflux condenser. The flask was immersed in an oil bath at 120 ^{0}C to boil the solution. For each material, a series of the samples was oxidized for different time ranging from 1 to 12 hours. After boiling the mixture was cooled to room temperature and filtered. The solid was washed on the filter with water until the filtrate was neutral, washed with 10 mL of methanol and 10 mL of DMF and redispersed in 40 mL of DMF by bath sonication for 60 min. The filtrates from all the nanotube materials were colorless.

Material balance. To estimate the loss of nanotubes during oxidation, 50 mg samples of all types of nanotubes were oxidized for different time using either of the described above protocols. The solids were filtered and dried at 100 ^{0}C to constant mass. The content of metal oxide and residual moisture was measured by TGA in air. According to the manufacturers the nanotube materials contained carbon and metal residue which was Mo in CoMoCat, Fe in HiPco and Co, Ni and Y in the weight ratio of 1:1:5 in PLV materials. For the calculations it was assumed that upon heating to 800 ^{0}C in the TGA experiment all carbon was converted into volatile oxides and the ashes contained MoO_3 from CoMoCat, Fe_2O_3 from HiPco and Co_3O_4 + NiO + Y_2O_3 from PLV materials.

Dispersability of oxidized SWNT. Carbon nanotubes in solvents never form true solutions but rather colloidal dispersions containing both individual tubes of various length and bundles consisting of various number of tubes. At higher concentrations bundles tend to form 3-dimensional aggregates.[35] The scientific literature describes a number of different methods for the evaluation of solubility of carbon nanotubes[33,36-38]. However, neither the term "solubility" nor a standard method for its determination has been established for this material. Here we define soluble nanotubes as a visually uniform dispersion in a solvent for a time of 2 hours or longer. We define the solubility as the highest weight percent of nanotubes that can be dispersed in 1 L of a solvent and no suspended particles can be visually observed. To evaluate the solubility, a dispersion of oxidized nanotubes was diluted with a solvent in 10 mL glass vials to yield a series of concentrations from 0.01 to 0.2 mg/L. Each vial was sonicated by the tip sonicator at 10 W for 15 min at room temperature and left on the bench for 2 hours, and the dispersions were examined for the presence of visible particles. The dispersions with concentration of ≥0.1 g/ L appeared black, so they were transferred into a 2 mm glass cell for better observation. The highest concentration of SWNT with no visible particles was used as a solubility value for a certain solvent. These values of the solubility are good for comparison among our samples and may vary from the values determined by other methods. In our samples at the solubility limit a black solid was visible on the bottom of the vial beginning about 3-4 hours after preparation, while the supernatant liquid remained homogeneous. The optical absorption of the dispersions left on the bench for 10 days reduced by 20–30 %. In the samples above the solubility limit, aggregation occurred in a few minutes after sonication, so the limit could be clearly established.

Results and Discussion

Overview of the results. Figure 1 reports solubility of three different types of nanotubes in DMF, methanol, and water after oxidation. The sonication protocol significantly increases solubility of all nanotubes after 1 hour. Longer treatment resulted only in a moderate solubility increase. The reflux procedure requires 2–4 hours to achieve the same effect.

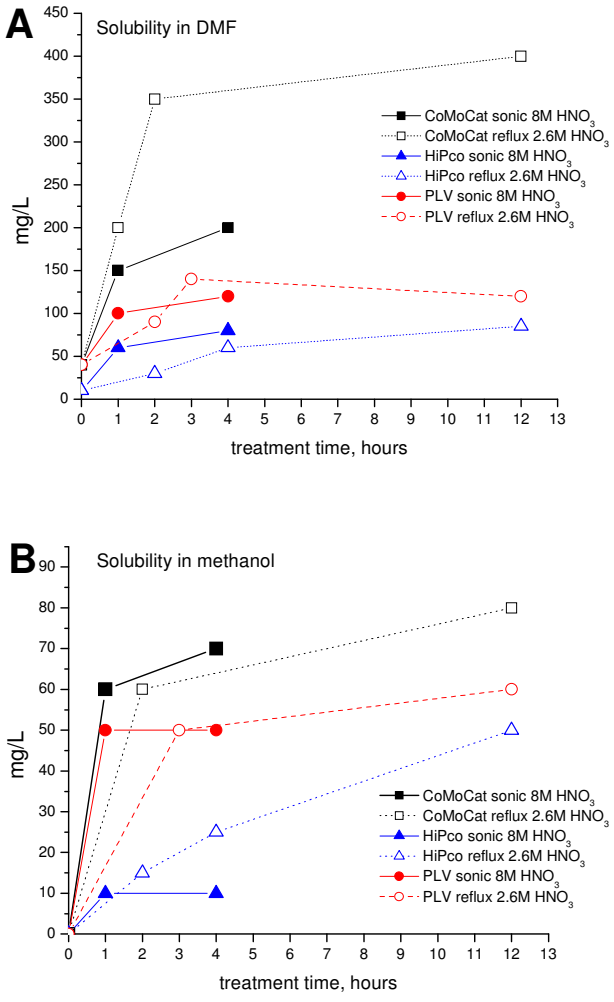

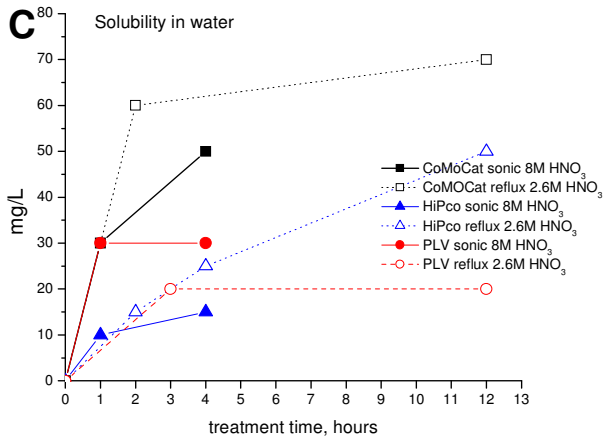

Figure 1. Solubility of oxidized nanotubes in the solvents: A – DMF; B – methanol; C – water.

Raman spectra in Figure 2 suggest chemical functionalization of the nanotubes as a result of nitric acid treatment. The degree of functionalization can be estimated by the relative intensity of the D-band (I_D) (arising due to defects in the structure of the nanotube sidewall) in respect to the intensity of the G-band (I_G) (corresponding to the stretching vibrations of the sp^2 carbons).[39]

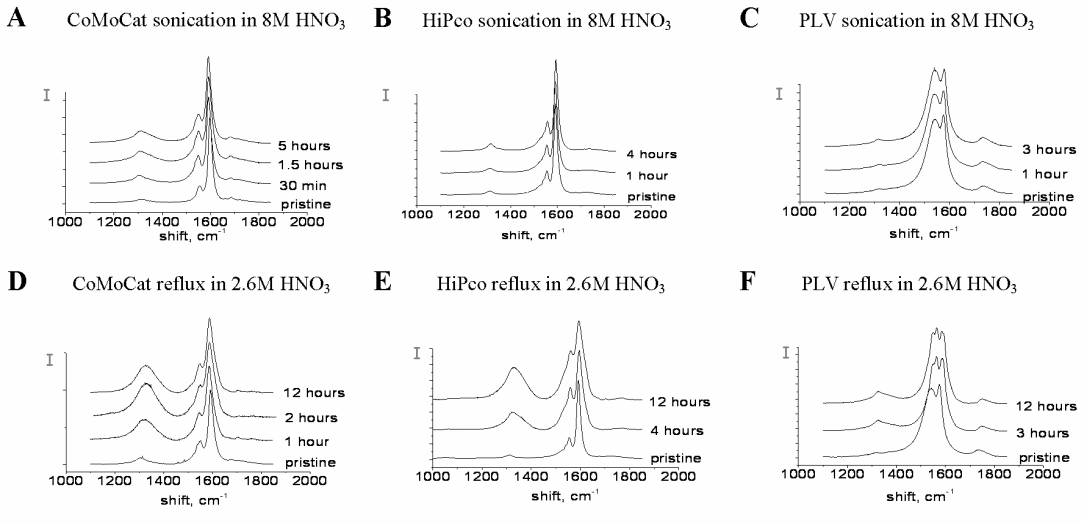

Figure 2. Raman spectra of the oxidized SWNT. The spectra have been normalized to the intensity of the G-band.

The appearance of polar groups on the surface of SWNT is responsible for the changes in solubility. AFM analyses revealed that oxidation increased the number of individual tubes and small bundles in solution (Figure 3). At the same time, oxidation leads to the shortening of nanotubes as can be seen in Figure 4. Prolonged treatment results in loss of nanotube material which is shown in Figure 5.

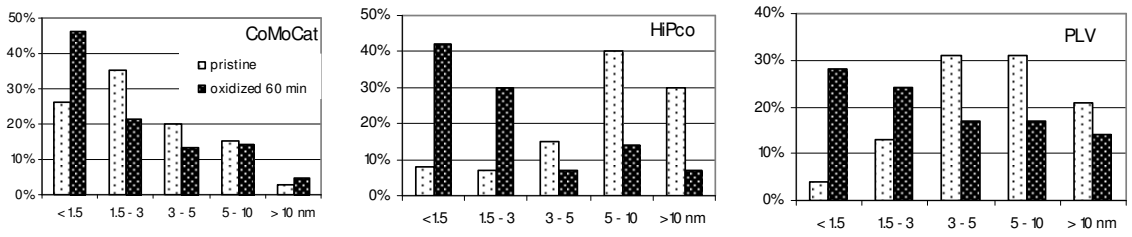

Figure 3. Diameter distribution for all 3 types of SWT before and after sonication in 8 M HNO_3 for 60 min, measured by AFM.

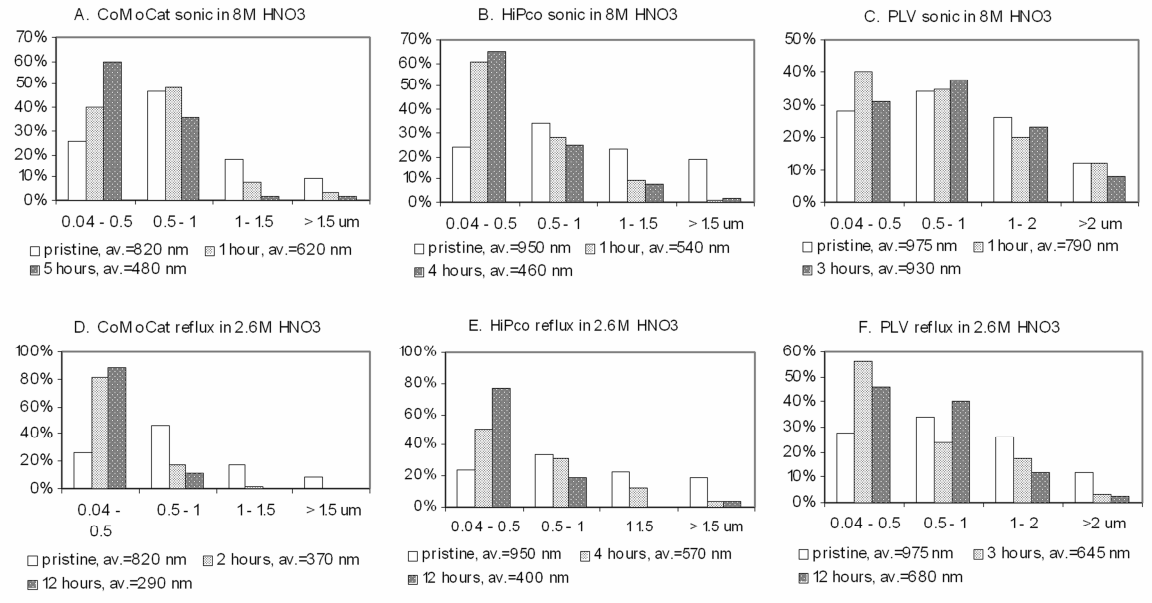

Figure 4. Length distribution within SWNT samples after oxidation, measured by AFM.

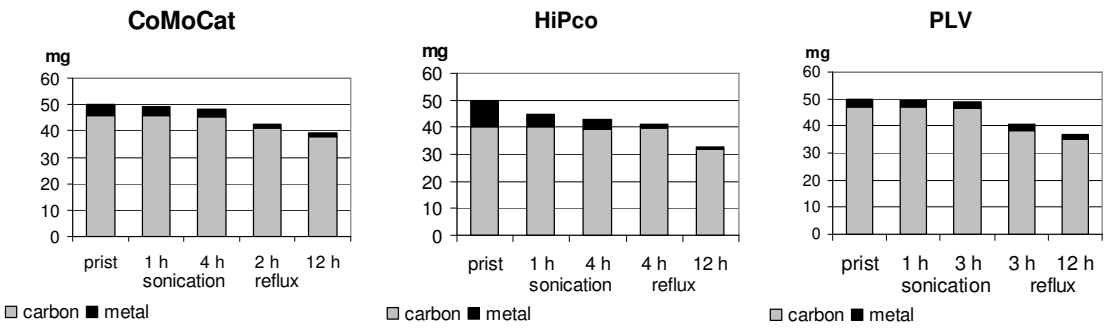

Figure 5. Material balance of nitric acid oxidation of SWNT, calculated from TGA.

The results of the AFM, Raman and TGA analyses for different samples of oxidized SWNT are presented in Table 1.

Table 1. Results of the AFM, Raman and TGA analyses for the SWNT samples.

SWNT material	Oxidation conditions	AFM Average length, nm	Raman I_D/I_G	TGA	
				Ratio of carbon/metal, %	Total material loss after oxidation, %
CoMoCat	Pristine	820	0.05	92.0/8.0	-
	Sonic 1 h	620	0.12	94.0/6.0	2.0
	Sonic 4 h	480	0.14	94.2/5.8	4.0
	Reflux 2 h	370	0.44	97.0/3.0	15.5
	Reflux 12 h	290	0.4	97.0/3.0	21.8
HiPco	Pristine	950	0.05	80.0/20.0	-
	Sonic 1 h	540	0.065	89.0/11.0	10.0
	Sonic 4 h	460	0.08	91.5/8.5	14.0
	Reflux 4 h	570	0.22	97.0/3.0	18.0
	Reflux 12 h	400	0.4	98.0/2.0	35.0
PLV	Pristine	975	0.07	94.0/6.0	-
	Sonic 1 h	790	0.08	95.0/5.0	1.0
	Sonic 3 h	930	0.09	95.0/5.0	2.0
	Reflux 3 h	645	0.15	94.4/5.6	19.2
	Reflux 12 h	680	0.18	95.0/5.0	24.4

Solubility of oxidized nanotubes. Zhang[4] investigated the effect of chemical oxidation on the structure of SWNTs using 3:1 concentrated H_2SO_4 (98 wt %)/HNO_3 (16 M) mixtures, diluted HNO_3 (2.6 M), and $KMnO_4$ and found that such oxidative procedures predominately create carboxylic acid functionalities on nanotubes. In the

work of Hu[29] the amount of carboxylic groups in SWNT refluxed in 3 M and 7 M HNO_3 was estimated by titration to be 6-11 % by mol, depending on the concentration of acid and time of treatment. The higher solubility of oxidized nanotubes in polar solvents should be attributed to the presence of the carboxylic groups. Changes in the I_D/I_G ratio in Raman spectra also suggest that chemical functionalization took place in all of the nanotube materials. However, in spite of continuous increase of this factor in HiPco and PLV nanotubes with the treatment time, the highest changes in solubility in DMF were observed in the first 3-4 hours of reflux or after 1 hour of sonication procedures, while longer treatment had only a little effect on solubility. This effect cannot be explained only by Raman spectroscopic results. It should be recalled that all pristine nanotubes contained some structural defects such as sp^3 carbons and localized double bonds, which are probably attacked first during oxidation. These defect sites have already contributed to the D-band so their oxidation should not increase its intensity. That's why both HiPco and PLV nanotubes oxidized for 1 hour by sonication protocol were already soluble in water despite a very low increase in the I_D/I_G. Hence, at the beginning of the process nitric acid facilitates exfoliation of bundles and oxidation of defects, thus giving the significant increase in solubility in DMF. Longer treatment moderately affects solubility mainly due to addition of new carboxylic groups to the sidewalls.

Solubility in water should be depended upon the presence of the charged groups at the nanotube sidewall. The results on solubility of oxidized SWNT in water correlate with the Raman spectra. CoMoCat material has the highest increase in I_D/I_G after 2 hours of reflux which results in the corresponding increase in solubility in water. For the PLV material the same effect is observed after 3 hours of reflux. In HiPco nanotubes, the D-

band grows proportionally to the time of reflux and therefore the solubility of this material in water grows linearly as well.

Despite a much higher degree of functionalization of the refluxed CoMoCat nanotubes, as judged by Raman spectra, there was no corresponding improvement in solubility in water for the refluxed samples compared to the sonicated samples. We attribute this phenomenon to the non-uniform distribution of the charged groups along the tubes. If the attack of nitric acid on the sidewalls breaks C-C bonds and introduces the carboxylic acid groups, oxidation may propagate from this site resulting in cutting the tube and having the charged functional groups on the edges of the cut. Shorter tubes have a higher fraction of functional groups on the ends, while aggregation may still be possible by stacking of the sidewalls. Unlike CoMoCat, HiPco nanotubes reveal linear increase in solubility in water and methanol with reflux time, which complies with a linear increase in D/G ratio of Raman spectra. A greater diameter of HiPco tubes than of CoMoCat tubes makes this material more stable against oxidation. If breaking the sidewall and introduction of an oxygen atom does not always result in cutting, we should expect more functional groups on the sidewalls of HiPco tubes and higher solubility in water.

Effect of nitric acid treatment on different types of nanotubes. Although nitric acid shortens and functionalizes all types of SWNT, each type reacts to a different extent. CoMoCat nanotubes express significant changes in the I_D/I_G in both sonication and reflux procedures, from 0.05 to 0.14 after 5 hours in sonication and to 0.4 after 12 hours in reflux. HiPco nanotubes are much less affected by acid in sonication, I_D/I_G changes from 0.05 to 0.08 after 4 hours, but the effect of reflux is more pronounced, from 0.05 to 0.4 after 12 hours. The sample refluxed for 24 hours showed even higher D-band intensity.

The PLV nanotubes were the least reactive in both procedures, judging by the I_D/I_G increase from 0.07 to 0.09 after 3 hours of sonication and to 0.18 after 12 hours of reflux. Similar results were obtained by optical absorption, as seen in Figure 6. In the CoMoCat samples, the interband transition peaks gradually diminished during 4 hours of ultrasonication in 8 M HNO_3 and completely disappeared after 1 hour of reflux in 2.6 M nitric acid. The UV-VIS spectra of HiPco material was practically unaffected by sonication protocol, and it took 12 hours of reflux to noticeably decrease the intensity of optical features in the spectra of these nanotubes. The spectra of the PLV samples were nearly unchanged in both protocols. Both Raman and UV-VIS absorption results suggest that the reactivity toward oxidation decreases in the row: CoMoCat > HiPco > PLV. This correlates with the average diameter of nanotubes in the samples, 0.8 nm for CoMoCat[40], 1.0 nm for HiPco,[41] and 1.3 nm for PLV.[42]

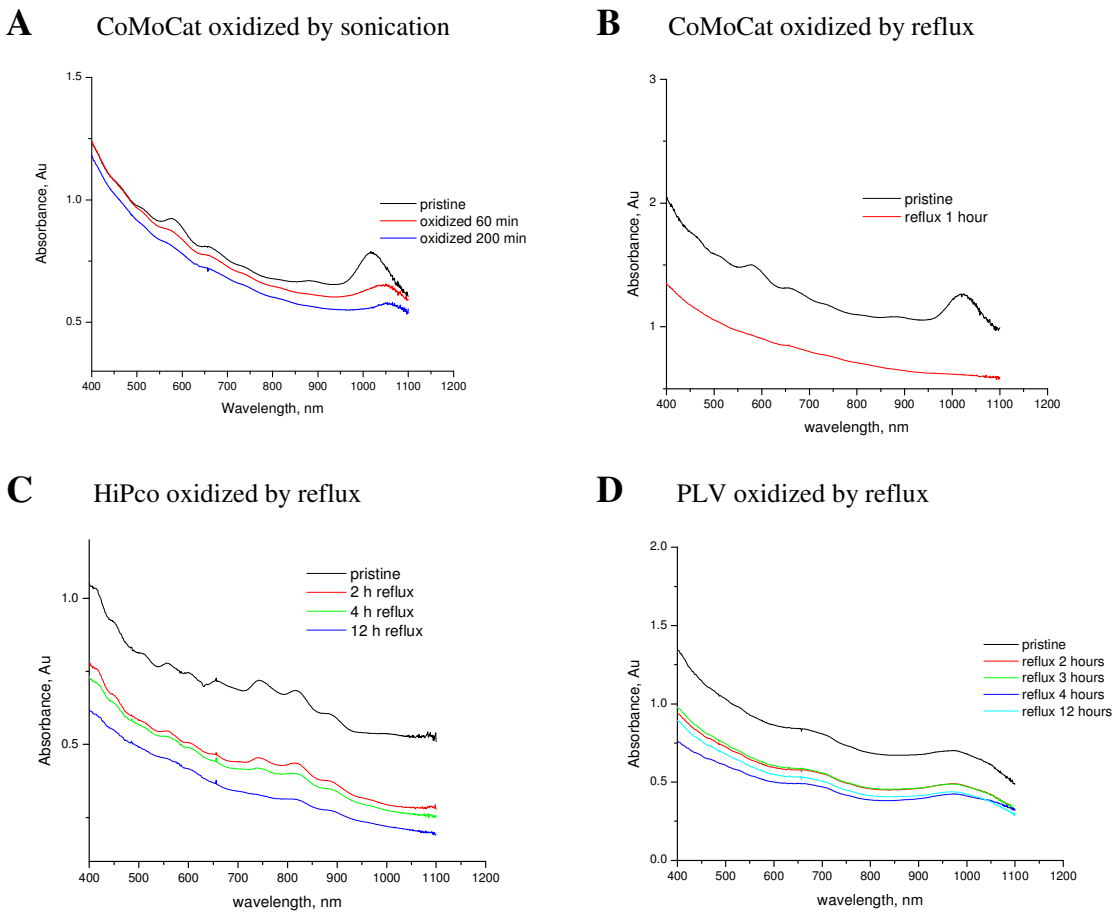

Figure 6. Optical absorption of the DMF dispersions of different SWNT samples.

The higher reactivity of smaller diameter nanotubes has been reported in the literature which has been explained by higher strain induced in the small nanotubes that leads to a greater chemical reactivity.[18,19,41,43] Figure 7 presents the RBM region of the Raman spectra of the oxidized CoMoCat SWNT. The peaks at 335, 309 and 285 cm^{-1}, corresponding to [6,4], [6,5] and [7,5] nanotubes,[44] are significantly reduced already after a short time of oxidation by refluxing HNO_3, indicating the preferential functionalization of these smaller diameter nanotubes respect to the other species in the sample. According to Jorio,[44] [6,5] and [7,5] nanotubes compose about 60% of the CoMoCat material (the peak of the [6,5] nanotube is not intense due to lack of resonance under 633 nm laser).

The Raman spectra of HiPco and PLV materials did not show a noticeable change in relative intensity of the RBM peaks after HNO_3 treatment.

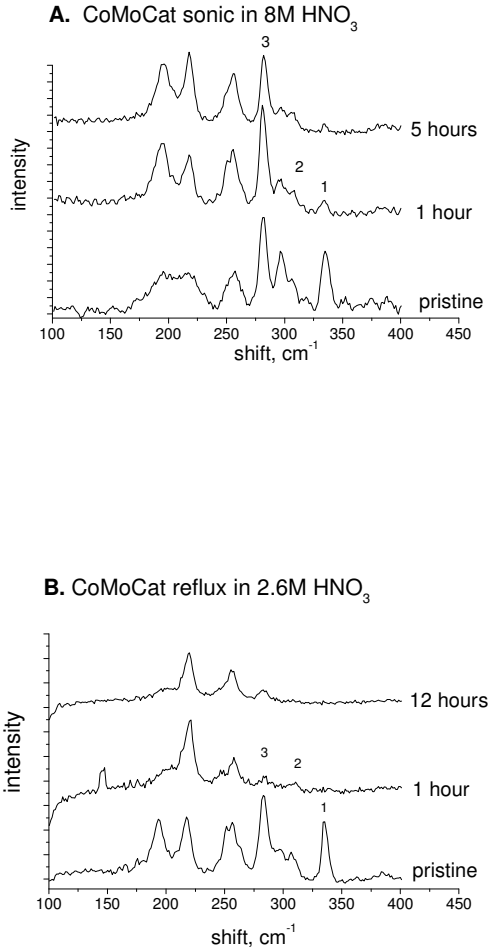

Figure 7. RBM region of Raman spectra of oxidized CoMoCat SWNT. The labeled peaks correspond to the nanotubes: 1 - [6,4]; 2 – [6,5]; 3- [7,5].

Zhang[4] proposed a mechanism of oxidation of the nanotube lattice in which acid initially attacks the defect sites such as localized double bonds and seven-membered rings. Stronger oxidation conditions facilitate addition to the six-membered rings as well. Further oxidation leads to breaking the graphene structure at the already generated active

sites and cutting the nanotube. According to Zhang the last two steps are possible only for strong oxidants such as concentrated nitric acid or $KMnO_4$. In contrast, our Raman and AFM analyses show that diluted nitric acid is also capable of breaking into the graphene structure and cutting the nanotubes. In small CoMoCat tubes, the maximum amount of new functionalities is probably introduced after 1.5 hours of sonication and after 2 hours of reflux, and further treatment results in cutting the tubes along these active sites. HiPco nanotubes, being larger in diameter and less reactive, seem to be more stable against cutting and allow accumulation of more defects at the sidewalls. PLV nanotubes, being the largest in the series, appear to be the most stable against oxidation. Compared to HiPco and CoMoCat materials, the covalent functionalization of the PLV nanotubes in significantly lower, as judged by Raman spectroscopy. Analyzing the PLV samples by AFM, it was noticed that the average length of the PLV tubes decreased during the first phase of oxidation but increases during the longer treatment. The length distribution (Figure 4 E and F) shows that such an increase was caused by disappearance of the short nanotubes in the mixture. In the other two materials, on the contrary, oxidation always results in a steady increase of the fractions of short tubes. The oxidative shortening of SWNT can occur by two mechanisms: breaking tubes into pieces and etching of tubes from the ends. If the first mechanism dominates, the material will have the fractions of short tubes increased, as it happens in CoMoCat and HiPco samples. In the PLV tubes, oxidation more likely proceeded by etching of the ends the tubes, since this material was found to be more stable against destruction of the sidewall lattice.

Shortening and loss of nanotubes during oxidation. Hu[17] found that reflux in 3 M and 7 M nitric acid for 12-48 hours led to an accumulation of carbonaceous impurities

and to the overall loss of material. The material loss increased with increased time of treatment or concentration of acid or temperature.[17,21,27] For the as-prepared Electric Arc SWNT, reflux in 3 M HNO_3 for 12 hours resulted in the loss of 31% of the material, 7% of which was carbon.[17] In our experiments, reflux in 2.6 M HNO_3 for 12 hours led to the 35% loss of as-prepared HiPco SWNT, 16% of which was carbon (Figure 5 and Table 1) Figure 5 also shows that sonication protocol is less destructive to nanotubes and results primarily in dissolution of metal residue and only in an insignificant loss of carbon. For HiPco SWNT the effect of 4 hours of either sonication or reflux was nearly identical. The next 8 hours of reflux resulted in a loss of the extra 15% of the material while the solubility in DMF increased only by 30%. At the same time, AFM analysis has shown the 30% decrease in average length of nanotubes for this period of time. For the CoMoCat SWNT, higher solubility in DMF and higher degree of functionalization were accompanied by greater shortening and loss of nanotubes. Therefore, if one chooses the oxidation conditions, the reasonable duration of treatment has to be considered. For instance, for the purposes of solubility the sonication protocol is preferable for all types of nanotubes, because less SWNT material is degraded to amorphous carbon material.

Conclusions

Based on the experimental data, the following conclusions can be made:

1. Mild nitric acid oxidation results in decreased diameter of bundles and increased solubility of single-walled carbon nanotubes in polar organic solvents and water. The major increase in solubility occurs after a short time of treatment (1 hour in sonication

and 2 to 4 hours in reflux) while a longer treatment time increased solubility only a slight amount.

2. Oxidation leads to shortening of nanotubes. The larger diameter PLV nanotubes were shortened less than HiPco and CoMoCat SWNT.

3. The reactivity of nanotubes toward oxidation appears to be inversely proportional to their diameter. PLV material was the least reactive due to the highest average diameter of tubes and the CoMoCat material has shown the highest reactivity. Within this material the smaller diameter nanotubes were found to react faster than others.

4. The reflux oxidation procedure is more destructive to nanotubes than the sonication procedure. Greater shortening and material loss were observed in the refluxed nanotubes whereas the gain in solubility compared to sonication protocol was minimal for most of the samples.

Oxidation of nanotubes is an important step toward further chemical functionalization. Functionalization is very useful in preparation of polymer composites of nanotubes with the goal of increasing mechanical strength or electrical conductivity of the polymer. Both of these properties are highly dependent on the nanotube length. Therefore the length control during oxidation is important. Based on the Raman spectroscopy and AFM microscopy, the most rational procedures for oxidation of nanotubes would be the following:

- CoMoCat SWNT: sonication in 8 M HNO_3 for 1.5 hours. The reflux procedure is especially harmful for this material.

- HiPco SWNT: reflux in 2.6 M HNO_3 for 4 hours. Reflux allows a higher degree of functionalization, however, the duration should not exceed this time to minimize shortening and material loss.
- PLV SWNT: sonication in 8 M HNO_3 for 12 hours is preferred if high solubility, long average length and small material loss are important.

Since every commercial SWNT material is a unique mixture of various types of nanotubes, the stepwise oxidation with monitoring of the size and structure by AFM and Raman is the best method for finding the right conditions for the process. In the current research, SWNT oxidized by sonication protocol were utilized for the preparation of composites with polystyrene by solution processing. Electrical properties of the composites are reported in Chapter IV of this dissertation.

References

(1) Lin, Y.; Meziani, M. J.; Sun, Y.-P. *J. Mater. Chem.* **2007**, *17*, 1143.

(2) Liu, J.; Rinzler, A. G.; Dai, H.; Hafner, J. H.; Bradley, R. K.; Boul, P. J.; Lu, A. Iverson, T.; Shelimov, K.; Huffman, C. B.; Rodriguez-Macias, F.; Shon, Y.-S.; Lee, T. R.; Colbert, D. T.; Smalley, R. E. *Science* **1998**, *280*, 1253.

(3) Martinez, M. T.; Callejas, M. A.; Benito, A. M.; Cochet, M.; Seeger, T.; Anson, A.; Schreibert, J.; Gordon, C.; Marhic, C.; Chauvet, O.; Fierro, J. L. G.; Maser, W. K. *Carbon* **2003**, *41*, 2247.

(4) Zhang, J.; Zou, H.; Qing, Q.; Yang, Y.; Li, Q.; Liu, Z.; Guo, X.; Du, Z. *J. Phys. Chem. B* **2003**, *107*, 3712.

(5) Hamon, M. A.; Chen, J.; Hu, H.; Chen, Y.; Itkis, M. E.; Rao, A. M.; Elkund, P. C.; Haddon, R. C. *Adv. Mater.* **1999**, *11*, 834.

(6) Tasis, D.; Tagmatarchis, N.; Bianco, A.; Prato, M. *Chem. Rev.* **2006**, *106*, 1105.

(7) Zhu, J.; Kim, J.; Peng, H.; Margrave, J. L.; Khabashesku, V. N.; Barrera E. V. *Nano Lett.* **2003**, *3*, 1107.

(8) Zhao, B.; Hu, H.; Haddon, R. C. *Adv. Funct. Mater.* **2004**, *14*, 71.

(9) Qin, S.; Qin, D.; Ford, W. T.; Resasco, D. E.; Herrera, J. E. *J. Am. Chem. Soc.* **2004**, *126*, 170.

(10) Hong, C.-Y.; You, Y.-Z.; Pan, C-Y. *Chem. Mater.* **2005**, *17*, 2247.

(11) Peng, H.; Alemany, L. B.; Margrave, J. L.; Khabashesku, V. N.; Barrera, E. V. *J. Amer. Chem. Soc.* **2003**, *125*, 15174.

(12) Dyke, C. A.; Tour, J. M. *Chem. Eur. J.* **2004**, *10*, 812.

(13) Liu, Y.; Yao, Y.; Adronov, A. *Macromolecules* **2005**, *38*, 1172.

(14) Mitchell, C. A.; Bahr, J. L.; Arepalli, S.; Tour, J. M.; Krishnamoorti, R. *Macromolecules* **2002**, *35*, 8825.

(15) Sen, R.; Zhao, B.; Perea, D.; Itkis, M. E.; Hu, H.; Love, J.; Bekyarova, E.; Haddon, R. C. *Nano Lett.* **2004**, *4*, 459.

(16) Rinzler, A. G.; Liu, J.; Dai, H.; Nikolaev, P.; Huffman, C. B.; Rodriguez-Macias, F. J.; Boul, P. J.; Lu, A. H.; Heymann, D.; Colbert, D. T.; Lee, R. S.; Fischer, J. E.; Rao, A. M.; Elkund, P. C.; Smalley, R. E. *Appl. Phys. A* **1998**, *67*, 29.

(17) Hu, H.; Zhao, B.; Itkis, M. E.; Haddon, R. C. *J. Phys. Chem. B* **2003**, *107*, 13838.

(18) Yang, Y.; Zou, H.; Wu, B.; Li, Q.; Zhang, J.; Liu, Z.; Guo, X.; Du, Z. *J. Phys. Chem. B* **2002**, *106*, 7160.

(19) Yang, C.; Park, J. S.; An, K.H.; Lim, S. C.; Seo, K.; Kim, B.; Park, K.A.; Han, S.; Park, C. Y.; Lee, Y. H. *J. Phys. Chem. B* **2005**, *109*, 19242.

(20) Miyata, Y.; Maniwa, Y.; Kataura, H. *J. Phys. Chem. B* **2006**, *110*, 25.

(21) Dillon, A. C.; Gennett, T.; Jones, K. M.; Alleman, J. L.; Parilla, P. A.; Heben, M. J. *Adv. Mater.* **1999**, *11*, 1354.

(22) Zhang, X.; Sreekumar, T. V.; Liu, T.; Kumar, S. *J. Phys. Chem. B* **2004**, *108*, 16435.

(23) Zhao, W.; Song, C.; Pehrsson, P. E. *J. Am. Chem. Soc.* **2002**, *124*, 12418.

(24) Ziegler, K. J.; Gu, Z.; Peng, H.; Flor, E.L.; Hauge, R. H.; Smalley, R .E. *J. Am. Chem. Soc.* **2005**, *127*, 1541.

(25) Cai, L.; Bahr, J. L.; Yao, Y.; Tour, J. M. *Chem. Mater.* **2002**, *14*, 4235.

(26) Mamedov, A. A.; Kotov, N. A.; Prato, M.; Guldi, D. M.; Wicksted, J. P.; Hirsch, A. *Nature Mater.* **2002**, *1*, 190.

(27) Martinez, M. T.; Callejas, M. A.; Benito, A. M.; Cochet, M.; Seeger, T.; Anson, A.; Schreibert, J.; Gordon, C.; Marhic, C.; Chauvet, O.; Fierro, J. L.G.; Maser, W. K. *Nanotechnology* **2003**, *14*, 691.

(28) Chen, J.; Rao, A. M.; Lyuksyutov, S.; Itkis, M. E.; Hamon, M. A.; Hu, H.; Cohn, R. W.; Elkund, P. C.; Colbert, D. T.; Smalley, R. E.; Haddon, R. C. *J. Phys. Chem. B* **2001**, *105*, 2525.

(29) Hu, H.; Yu, A.; Kim, E.; Zhao, B.; Itkis, M. E.; Bekyarova, E.; Haddon, R. C. *J. Phys. Chem. B* **2005**, *109*, 11520.

(30) Kityanan, B.; Alvarez, W. E.; Harwell, J. H.; Resasco, D. E. *Chem. Phys. Lett.* **2000**, *317*, 497.

(31) Dai, H.; Rinzler, A. G.; Nikolaev, P.; Thess, A.; Colbert, D. T.; Smalley, R. E. *Chem. Phys. Lett.* **1996**, *260*, 471.

(32) Arepalli, S.; Nikolaev, P.; Holmes, W.; Files, B. S. *Appl. Phys. Lett.* **2001**, *78*, 1610.

(33) Matarredona, O.; Rhoads, H.; Li, Z.; Harwell, J. H.; Balzano, L.; Resasco, D. E. *J. Phys. Chem. B* **2003**, *107*, 13357.

(34) Nikolaev, P., Gorelik, O., Allada, R. K., Sosa, E. Arepalli, S. and Yowell, L. *J. Phys. Chem. C,* **2007**, *111,* 17678..

(35) Bauer, B. J.; Becker, M. L.; Bajpai, V.; Fagan, J. A.; Hobbie, E. K.; Migler, K.; Guttman, C. M.; Blair, W. R. *J. Phys. Chem. C* **2007**, *111,* 17914.

(36) Bahr, J. L.; Mickelson, E. T.; Bronikowski, M. J.; Smalley, R. E.; Tour, J. *Chem. Commun.* **2001**, *2*, 193.

(37) Rouse, J. H. *Langmuir* **2005**, *21*, 1055.

(38) Moore, V. C.; Strano, M. S.; Haroz, E. H.; Hauge, R. H.; Smalley, R. E.; Schmidt, J.; Talmon, Y. *Nano Lett.* **2003**, *3*, 1379.

(39) Thomsen, C.; Reich, S. *Phys. Rev. Lett.* **2000**, *85*, 5214.

(40) Bachilo, S. M.; Balzano, L.; Herrera, J. E.; Pompeo, F.; Resasco, D. E.; Weisman, R. B. *J. Am. Chem. Soc.* **2003**, *125*, 11186.

(41) Zhou, W.; Ooi, Y. H.; Russo, R.; Papanek, P.; Luzzi, D. E.; Fischer, J. E.; Bronikowski, M. J.; Willis, P. A.; Smalley, R. E. *Chem. Phys. Lett.* **2001**, *350*, 6.

(42) Yudasaka, M.; Sensui, N.; Takizawa, M.; Bandow, S.; Ichihashi, T.; Iijima, S. *Chem. Phys. Lett.* **1999**, *312*, 155.

(43) Zhang, M.; Yudasaka, M.; Iijima, S. *J. Phys. Chem. B* **2004**, *108*, 149.

(44) Jorio, A.; Santos, A. P.; Ribeiro, H. B.; Fantini, C.; Souza, M.; Vieira, J. P. M.; Furtado, C. A.; Jiang, J.; Saito, R.; Balzano, L.; Resasco, D. E.; Pimenta M. A. *Phys. Rev. B* **2005**, *72*, 075207/1.

CHAPTER V

COMPOSITES OF SWNT AND POLYSTYRENE: PREPARATION AND ELECTRICAL PROPERTIES

Abstract

Composites of single-walled carbon nanotubes and polystyrene have been prepared using three different materials: HiPco™, CoMoCat™ and Pulsed Laser Vaporization (PLV) SWNT. Two methods of incorporation of nanotubes in the polystyrene matrix have been explored: (1) evaporation of the chloroform solutions of SWNT non-covalently functionalized with poly[(*m*-phenylenevinylene)-*co*-(2,5-dioctoxy-*p*-phenylenevinylene)] (PmPV) and polystyrene; and (2) coagulation of the DMF solutions of nitric acid oxidized SWNT and polystyrene in water. Electrical conductivity of the resulting composites with different loading of nanotubes has been measured. The percolation threshold for conductivity was 0.17-0.3 weight % SWNT for the evaporated materials and 0.5-0.8 weight % for those made by coagulation due to a lower aspect ratio of the bundles of oxidized nanotubes. The composites of HiPco SWNT had the highest conductivity at the plateau region among the three materials. The conductivity versus SWNT loading obeyed the power law with the critical exponent of 2.0-4.8 for different samples. This parameter was higher for the composites of oxidized nanotubes.

Introduction

Carbon nanotubes are novel synthetic materials possessing a number of exceptional physical properties, such as high mechanical strength, high electrical and thermal conductivity, as well as unique optical and electronic properties. All such properties make carbon nanotubes unrivaled for a wide range of applications. Electrical conductivity of individual bundles of metallic carbon nanotubes reaches the value of 10^4 S/cm[1] which is close to that of metals (59×10^4 S/cm for copper and 9.9×10^4 S/cm for iron), while the density of nanotubes is much lower. These properties make carbon nanotubes excellent candidates to incorporate with polymers for production of conductive composites for electrostatic dissipative materials as well as other useful components in electronics.

The percolation theory suggests that the conductivity σ of a composite depends on the volume fraction of a filler f through the following equation:[2]

$$\sigma = C(f - f_c)^{\beta}, \qquad (1)$$

where f_c is the volume fraction at the percolation threshold, **C** is a constant, and **β** is the critical exponent which reflects percolation mechanism. The theoretical value of β for the three-dimensional isotropically random binary systems has been estimated to be 1.6-2.[3,4] Sometimes volume fraction is substituted by mass fraction. Since in the nanotube-polymer composite the electric current is carried out only through the network of nanotubes, one should expect that the better the nanotubes are distributed in the polymer, the lower the fraction of them is needed for the percolation. Hence, in order to achieve a high electrical conductivity at low CNT loadings, a small bundle size and a uniform distribution of nanotubes in the composites are important.

Table 1 summarizes the data on the electrical properties of the nanotube-polymer composites published in the literature since 1998 and shows different approaches for the preparation of composites. The term "plateau region" in this table refers to the region of the log(σ) versus mass fraction plot where the changes of the log(σ) become minimal. Literature data suggest that the percolation threshold f_c is dependent both on the type of nanotubes and polymer and on the preparation method. The lowest f_c values have been achieved for the epoxy resin composites, probably because of the low viscosity of this material. Based on Table 1, three basic approaches to the preparation of composites can be described: blending of nanotubes with the molten polymer, polymerization of the monomer in the presence of nanotubes, and mixing nanotubes and polymer in solution, followed by retrieving the solid via different ways. The latter two methods show the better results because such allow the better distribution of nanotubes in the polymer matrix. The composites prepared by spin-coating or casting of thin films from solutions generally revealed lower percolation threshold than those prepared by coagulation. However, the casting method is capable of obtaining only thin films of the composite and is good only for testing but not for practical materials. For larger amount of material with uniform orientation of nanotubes the solvent can be removed by evaporation (or boiling) under vacuum. This method is most efficient for a volatile and low-boiling solvent such as chloroform. In the case of a high-boiling solvent, evaporation takes a long time and nanotubes aggregate as the dispersion becomes more concentrated. For such a solvent, coagulation of dispersion into a large amount of a non-solvent is preferable because rapid removal of the solvent leaves the nanotubes "trapped" inside of the polymer particles.

Table 1. Electrical properties of different carbon nanotube – polymer composites.*

Nanotubes	Polymer	Method of preparation	Weight percent at the percolation threshold, %	Conductivity at the plateau region, S/cm	Reference
MWNT	epoxy resin	mixing with resin followed by curing	0.0025	10^{-3}	Sandler[5]
PLV and HiPco SWNT	epoxy resin	mixing with resin followed by curing	PLV: 0.0052 %(vol) HiPco:0.0085 %(vol)	Laser: 10^{-6} HiPco: 10^{-7}	Brynning[6]
HiPco SWNT	PS (PPE addition)	spin-coating from solution	0.045	0.05 - 0.1	Ramasubramaniam[7]
CVD SWNT	epoxy resin	mixing with resin followed by curing	0.05	10^{-4}	Gojny[8]
PLV SWNT	polyimide	in-situ polymerization	0.05	10^{-7}	Ounaies[9]
HiPco SWNT	PC (PPE addition)	spin-coating from solution	0.11	2.0 - 5.0	Ramasubramaniam[7]
MWNT	polyimide	in-situ polymerization	0.15 %(vol)	10^{-3}	Jiang[10]
HiPco SWNT	PMMA	casting from solution	0.17	10^{2} (for the SOCl2 doped CNT)	Skakalova[11]
CoMoCat SWNT	PS-co-PI	mixing of aqueous emulsions of CNT and polymer	0.2	10^{-6}	Ha[12]
HiPco SWNT	PBT	in-situ polymerization	0.2	n/a	Nogales[13]
EA SWNT	PS	casting from solution	0.27	10^{-5}	Chang[14]
EA SWNT	PS	mixing of aqueous emulsions of CNT and polymer	0.3	10^{-3}	Grossiord[15]
HiPco SWNT	PMMA	coagulation from solution	0.39	10^{-4}	Du[16]
EA and HiPco SWNT	PC	coagulation from solution and blending in extruder	0.8 (for coagulation), 1.7 (for blending)	10^{-2}	Hornbostel[17]
MWNT	PP	high shear mixing in molten polymer	1.5	10^{-3}	Seo[18]
MWNT	LLDPE	mixing in molten polymer	2	10^{-2}	Gorrasi[19]
MWNT	PE	blending in extruder	7.5	10^{-6}	McNally[20]
EA SWNT	PmPV	spin-coating from solution	8.4	10^{-3}	Coleman[21]

* Abbreviations: PLV – pulse laser vaporization, EA – electric arc discharge, CVD – chemical vapor deposition, PS – polystyrene, PPE – poly(phenyleneethynylene), PC – polycarbonate, PMMA – poly(methyl methacrylate), PI – polyisoprene, PBT – poly(butylene terephtalate), PP – polypropylene, LLDPE – linear low density polyethylene, PE – polyethylene, PmPV – poly(*p*-phenylenevinylene-co-2,5-dioctoxy-*m*-phenylenevinylene).

In the present work three types of single-walled carbon nanotubes were used, produced by HiPco,[22] CoMoCat[23] and Pulse Laser Vaporization[24] (PLV) protocols to prepare composites with polystyrene by two different methods. First, the nanotubes were dispersed in chloroform with the aid of poly[(m-phenylenevinylene)-*co*-(2,5-dioctoxy-*p*-phenylenevinylene)] polymer (PmPV). Ability of this copolymer to form stable dispersions of SWNT in chloroform at concentrations as high as 1.2 g/L has been demonstrated by Star.[25] Chen[26] has used a poly(phenyleneethynylene) (PPE), a copolymer similar to PmPV, for solubilizing SWNT in chloroform and has shown that this polymer is more efficient than PmPV for the small diameter nanotubes. Ramasubramaniam[7] utilized the PPE polymer to prepare composites with polystyrene by spin-coating. In the present work, rotary evaporation under vacuum was employed to remove the chloroform from the composite.

The second method of composite preparation was precipitation of the mixture of polystyrene and a dispersion of the nanotubes (oxidized by nitric acid) from DMF into water. We have shown in Chapter 3 that sonication of nanotubes in 8 M nitric acid for 60 min significantly increased their solubility in DMF while preserving the electronic structure of nanotubes.

Experimental

Materials. Single-walled carbon nanotubes produced by CoMoCat,[23] HiPco[22] and pulsed laser vaporization (PLV)[24] processes were used in this work. CoMoCat nanotubes in the form of a 2% aqueous gel, grade S-P94-02gel, batch # OSU-A-007, purified by the basic (alkali) protocol[27] were obtained from Southwest Nanotechnologies, Inc., Norman,

OK. As-produced HiPco material in the form of a puffy fibrous powder, lot # R0488, was obtained from Carbon Nanotechnologies, Inc., Houston, TX. Laser oven SWNT (PLV) in the form of a black powder, batch # JSC-338, purified by the soft-baking protocol[28] was obtained from NASA Johnson Space Center, Houston, TX. PmPV copolymer was obtained from Aldrich. The molecular weight and polydispersity, as estimated by SEC chromatography using THF and polystyrene standards, were 3700 g/mol and 1.4, respectively. A sample of polystyrene of industrial grade, $M_w = 2x10^5$, $M_w/M_n = 3.6$, was used for composites. All the solvents were obtained from Pharmco and Spectrum and were dried over anhydrous potassium carbonate. All other chemicals were obtained from Sigma and Aldrich.

Instruments and measurements. Ultrasonication was performed using a Fisher FS-30 160W 3QT ultrasonic cleaner or a Microson XL-2000 22 KHz ultrasonic cell disruptor. Filtration of the solutions was done using a vacuum glass filtration cell and 0.45 μm porous PTFE or PP membranes. Atomic force micrographs were obtained using a Multimode Nanoscope IIIa SPM (Digital Instruments, Santa Barbara, CA) operating in the tapping mode. The samples were prepared by applying a drop of a suspension on a mica chip for a short time (10 min for DMF solutions and 10 sec for $CHCl_3$ solutions), followed by removing the liquid and drying the substrate in the nitrogen flow. Electrical conductivities were tested by two-probe method using a Keithley 610C Electrometer and a specially constructed resistivity chamber. The samples of composites were pressed into 15x15x0.5 mm pieces using a heat press and a custom made picture frame mold. The sample in the mold was heated up to 175 °C, followed by applying the 10,000 psi pressure for 1 min, releasing the pressure, taking the mold out of the press and cooling it

on the bench. Cooling the sample under continuous pressure showed no difference in the conductivity. Pressing the samples at 140 °C was also tested but resulted in the lower conductivity values, probably because the higher viscosity of the polymer prevented the sufficient homogenizing of the sample during the pressing. Two plastic pieces for each sample were prepared. Each piece was measured in 6 spots (3 spots on each side) resulting in 12 data points for each sample. In order to calculate the percolation threshold, the equation (1) was transformed into a linear form of y = ax+b by taking logarithms of the two parts:

$$\log(\sigma) = \beta * \log(m-m_c) + \log(C) \qquad (2)$$

In this equation, the volume fraction of the filler is substituted by mass fraction, assuming the equal density for all SWNT materials. The values for m_c, β, and C were calculated from the linear regression analysis. Thin films (50 ± 10 μm) of the composites for microscopy and spectroscopy were pressed using the same press and conditions. Optical microscopy of the films was performed on a Leica DM IRB optical microscope at 100x magnification. The UV-VIS spectroscopy of the films and organic dispersions was obtained on the Cary-5000 UV-VIS-NIR spectrometer in the wavelength range of 200-2000 nm. Thermogravimetric analyses were performed using a Shimadzu TGA50/50H instrument in air. Scanning electron microscopy was performed on a JEOL JSM 6400 Scanning Electron Microscope operating at 20-30 kV accelerating voltage. The samples were not coated by metal.

Solubility of SWNT in chloroform with the aid of PmPV. PmPV copolymer was soluble in THF, toluene, and chloroform and poorly soluble in DMF. Among all the solvents, only chloroform allowed stable dispersions of carbon nanotubes. To estimate

solubility of SWNT, stock dispersions containing 0.5 g/L of nanotubes and PmPV at the concentration of 0.5, 1.0, 1.5 and 2.0 g/L in chloroform were sonicated in bath for 60 min and stirred for 24 hours. All of the dispersions looked black. Observation through a 2 mm glass cell revealed small suspended particles. These stock dispersions were diluted with chloroform, yielding a series of dispersions with the SWNT concentration from 0.01 to 0.3 g/L and were transferred to 12 mL glass vials. The vials were immersed into water at 20 °C, sonicated by tip-sonicator for 15 min at the power of 15 W and left for 2 hours, after which time the liquid was examined for the presence of visible particles. If particles were not observed, the solution was considered to be uniform. For some of the uniform solutions, a black sediment was formed on the bottom after 8-10 hours. The sediment could be redispersed simply by shaking of the vial. For the solutions where concentration of nanotubes was much lower than the solubility limit, the uniform dispersion could be obtained by diluting the stock dispersion and vigorous shaking of the liquid for 5-6 sec, whereas for the SWNT concentrations close to the solubility limit always required sonication to make the dispersion uniform. For the solutions above the solubility limits, the longer sonication (up to 40 min) did not help to make them uniform.

SWNT/PmPV/PS composites. A stock dispersion containing 0.5 g/L of SWNT and 2.0 g/L of PmPV in chloroform was diluted by 1:5 with chloroform and sonicated in bath for 60 min. Water in the bath was replaced frequently in order to avoid heating of the dispersion. A 40 g/L solution of polystyrene in chloroform was prepared separately. The dispersion of SWNT was mixed with the solution of polystyrene in a ratio yielding the required proportion of nanotubes and polystyrene. The mixture was stirred for 1 hour followed by sonication by tip-sonicator for 15 min at 15 W at room temperature. The

mixture was replaced into a 250 mL round-bottom flask and the solvent was evaporated on the rotary evaporator. Residual solvent was removed under vacuum at 50 °C for 60 min. The final solid was dried at 110 °C for 1 hour.

Composites of oxidized SWNT and polystyrene. The nanotubes were oxidized by sonication in 8 M nitric acid for 60 min, followed by washing out the acid according to the previously reported procedure.[29] Oxidized nanotubes were dispersed in DMF at 0.5 g/L by sonication for 1 hour and stirring for 24 hours. The resulted dispersion was diluted with DMF by 1:10 and sonicated in bath for 60 min. Water in the bath was replaced frequently in order to avoid heating of the dispersion. The 20 g/L solution of polystyrene in DMF was prepared separately. Dispersion of SWNT was mixed with solution of polystyrene in a ratio, yielding the required proportion of nanotubes and polystyrene. The mixture was stirred for 1 hour, followed by sonication in bath for 30 min. The resulted mixture was precipitated by pouring into a 10-fold volume of water vigorously mixed with a mechanical stirrer, followed by filtration, washing the solid with water and methanol, and drying at 110 °C for 1 hour.

Composites of the polystyrene-functionalized SWNT and polystyrene. The sample of oxidized HiPco SWNT functionalized with polystyrene and separated from the unattached polymer (sample $SWNT_O$-PS from Chapter II B) in the form of 0.5 g/L dispersion in DMF was used for the composites. Composites were prepared by the solution mixing procedure identical to the described above for the composites of oxidized SWNT and polystyrene.

Results and Discussion

Composites of SWNT/PmPV/polystyrene. Figure 1 shows the solubility of different nanotubes in chloroform in the presence of PmPV. For the concentrations of SWNT and PmPV below the lines, the dispersions were uniform while for the concentrations above the lines they had visible suspended particles. These dispersions were obtained by diluting a more concentrated stock dispersion. Attempts to disperse nanotubes starting with low concentrations of SWNT and PmPV have failed. For example, dilution of the mixture of 0.5 g/L HiPco SWNT and 2 g/L of PmPV by 1:5 with chloroform, followed by 15 min of sonication, resulted in a uniform dispersion. However, dispersing 10 mg of HiPco and 40 mg of PmPV in 100 mL of chloroform did not result in uniform dispersions regardless of the sonication time, while the final concentration of components in both mixtures was the same. We attribute this phenomenon to adsorption of PmPV on the surface of SWNT. Adsorption is generally described by the Langmuir isotherm, where the surface coverage G_P (amount of solute adsorbed per unit of adsorbent) increased with the increased concentration of solute C in accordance with the equation:[30]

$$G_P = G_{PS}bC/(1+bC), \qquad (3)$$

We have estimated that concentrations of PmPV in chloroform of 0.5 g/L and higher were sufficient for obtaining uniform dispersions of SWNT after dilution, which indicates sufficient adsorption of the copolymer. Figure 1 also suggests that in order to increase concentration of nanotubes in dispersion, while keeping the dispersion uniform, the ratio

of PmPV to SWNT has to be increased too. Approximately, increasing the concentration of SWNT by 2 fold requires increasing the concentration of PmPV by 4 fold.

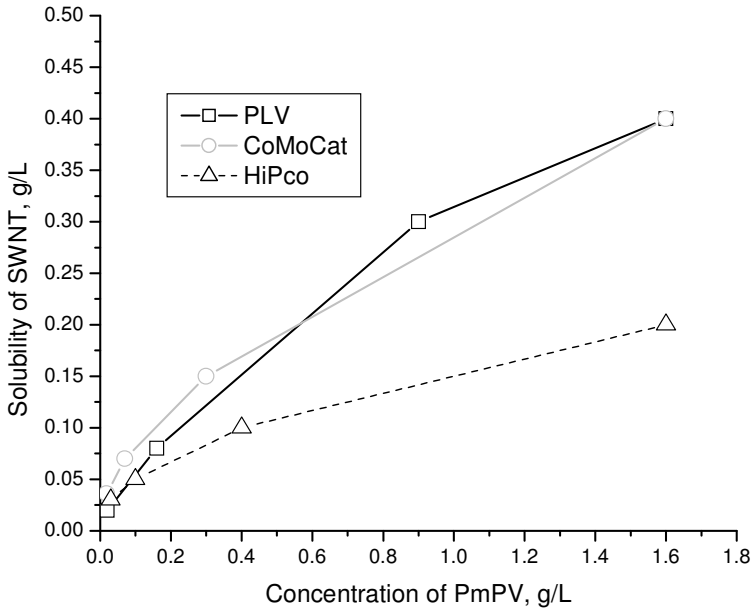

Figure 1. Dependence of the solubility of the SWNT in chloroform on concentration of the PmPV copolymer in the mixture.

Figure 2 presents AFM micrographs of pristine and PmPV-functionalized nanotubes. The length and height distribution of bundles in the AFMs measured by Section Analysis is given in Figure 3. In the PmPV-functionalized samples over 80% of the bundles were less than 10 nm in diameter with averages of 3.3 nm for HiPco, 3.1 nm for CoMoCat and 4.6 nm for PLV SWNT.

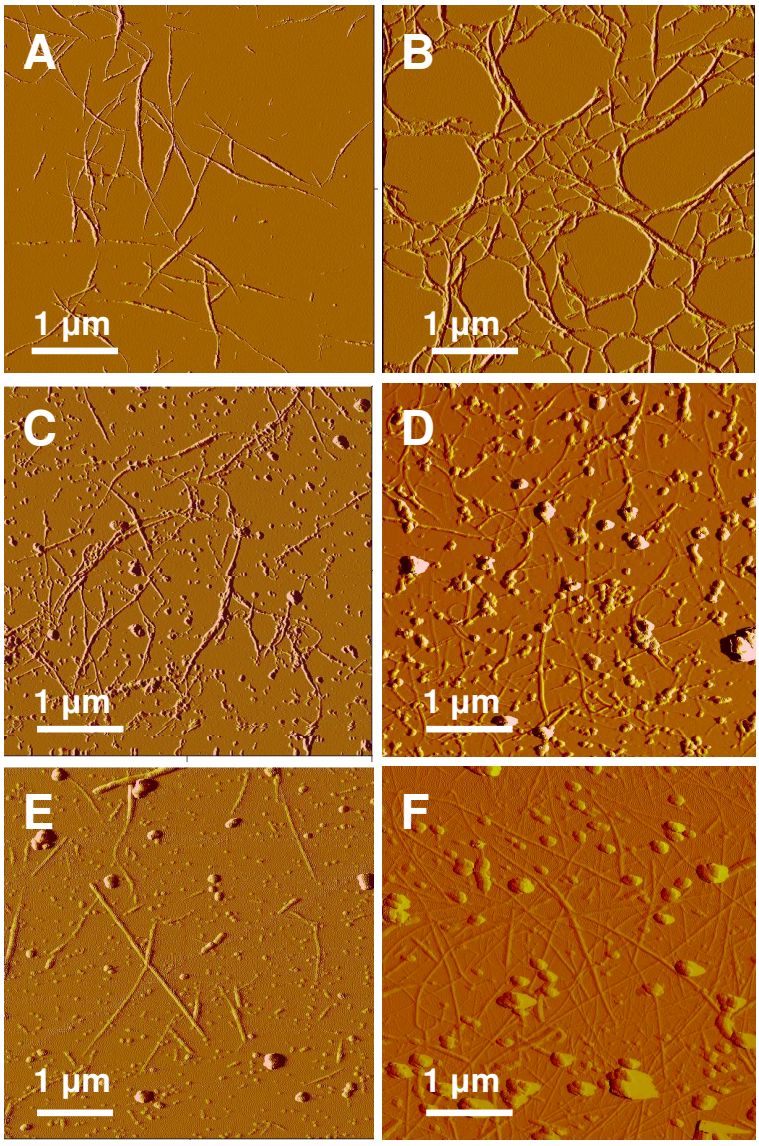

Figure 2. AFM of the pristine and PmPV-functionalized SWNT. A, C, E: pristine HiPco (A), CoMoCat (C) and PLV (E). B, D, F: PmPV-functionalized HiPco (B), CoMoCat (D) and PLV (F).

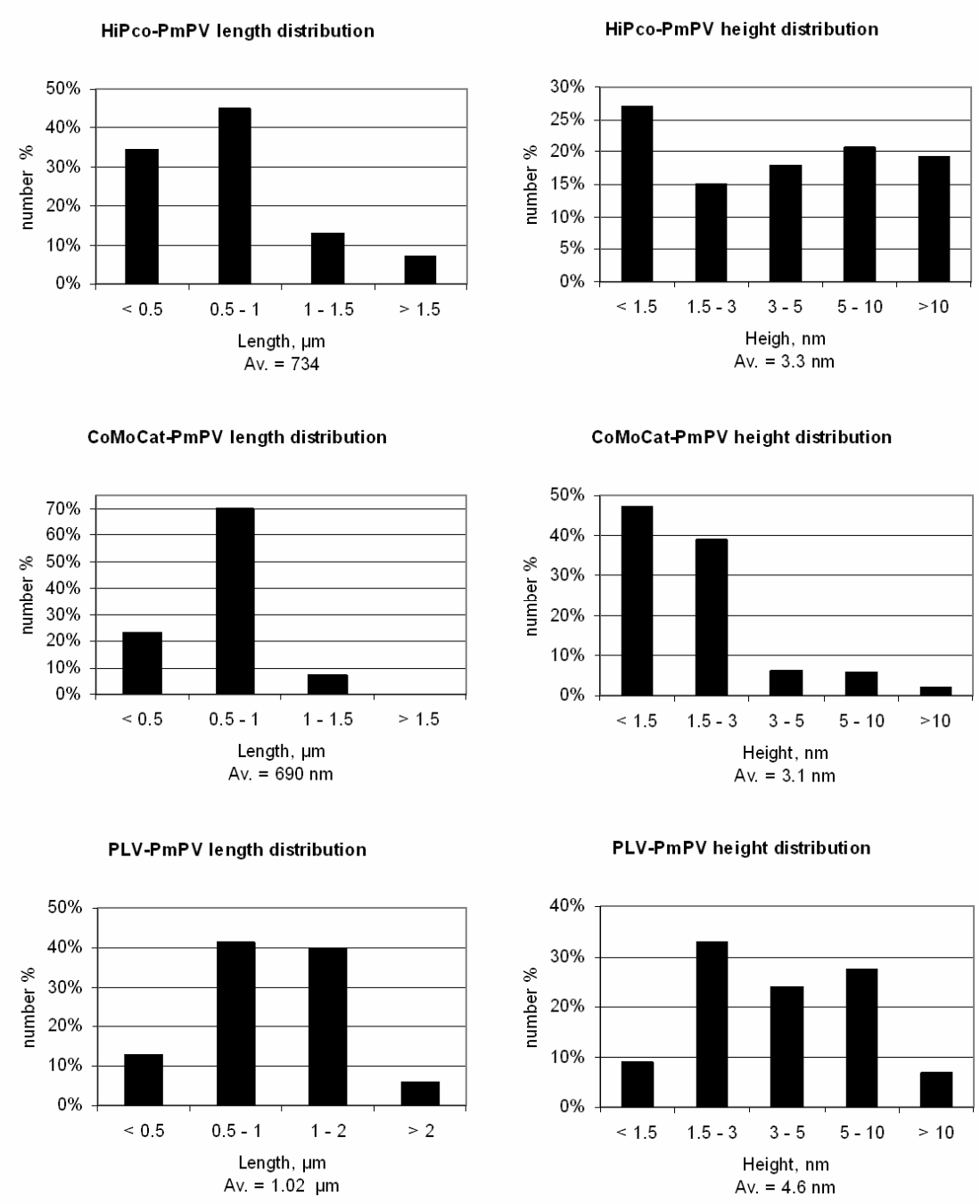

Figure 3. Length and diameter distribution in the samples of SWNT-PmPV, calculated from AFM.

The AFM of HiPco SWNT shows almost entirely tubular objects. Globular particles appear on the images of the CoMoCat and PLV materials in both pristine and

functionalized form, which suggests that these particles arise initially from the pristine materials. According to the manufacturer's information the PLV sample contained 20% to 25% of amorphous carbon, which was supported by TGA and SEM. TGA and SEM of the HiPco and CoMoCat SWNT did not provide an evidence for the presence of amorphous carbon in these CNT materials. High resolution SEM presented in Figure 4 revealed that globular particles in the CoMoCat SWNT are composed of aggregates of short nanotubes.

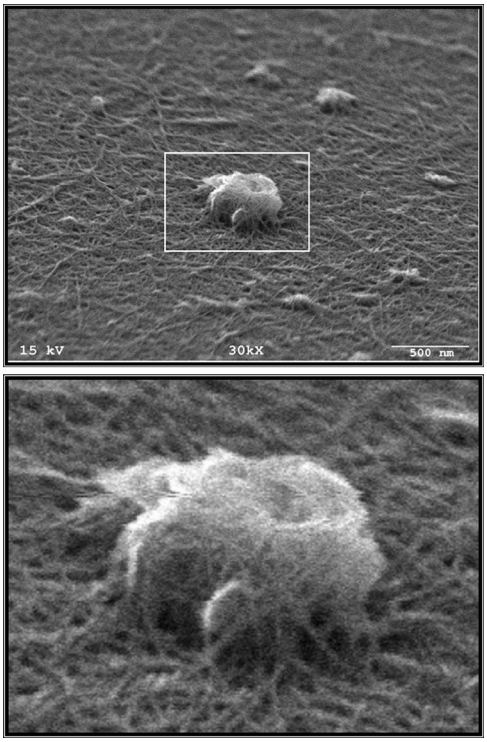

Figure 4. SEM of typical pristine HF-washed CoMoCat SWNT. Bottom image – zoomed area in the rectangle. Courtesy of Prof. D. E. Resasco, University of Oklahoma.

Figure 5 shows optical and Scanning Electron micrographs of the SWNT-PmPV-polystyrene composites. On the optical microscopic images of the HiPco composite the black tubular objects 5-10 μm long and about 1 μm thick can be attributed to the

aggregates of nanotubes. As for the CoMoCat and PLV composites, large aggregates of 5–20 μm in size appeared. SEM images show that such aggregates are composed primarily of nanotubes. These results point out that SWNT are not distributed evenly throughout the sample. The SEM of the composites was performed on the non-coated samples, which allowed imaging nanotubes inside the polymer matrix. However, due to scattering of electrons by the solid, only nanotubes located 50 nm and less from the surface could be observed in this microscopy technique, as suggested by Loose.[31]

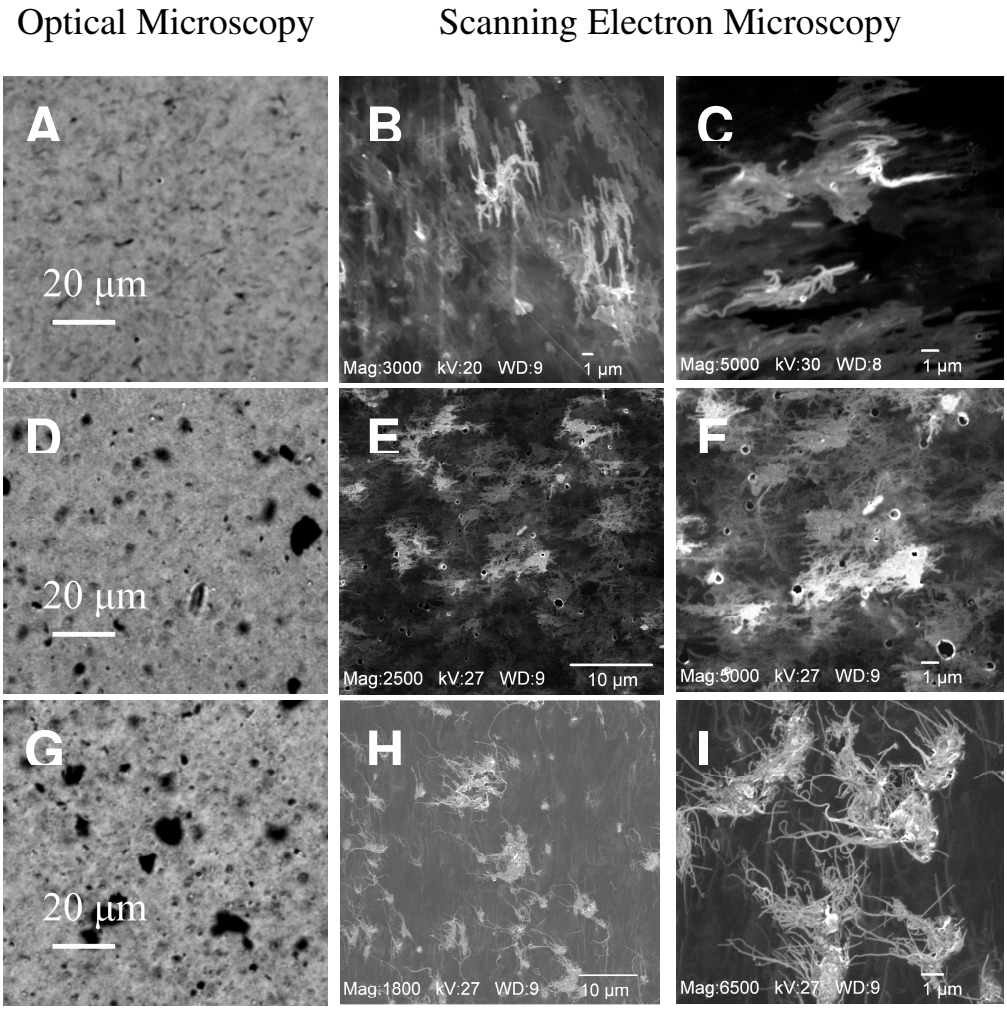

Figure 5. Optical microscopy (A, D, G) and SEM (the others) images of the SWNT-PmPV-PS composites of HiPco (A, B, C), CoMoCat (D, E, F) and PLV (G, H, I) materials.

Figure 6 (A, B, C) shows the optical absorption spectra of the PmPV-functionalized nanotubes acquired from solutions and from solid films of composites. The spectra were normalized at 800 nm for CoMoCat, 100 nm for HiPco, and 1300 nm for PLV, because of an absence of major interband transition peaks at these wavelengths for the corresponding materials. The sharpness of the peaks, expressed as the height to width ratio indicated the dispersion state of nanotubes, bundling reduces the sharpness.[32] The peaks from solid films appeared as sharp and distinct as those from solutions which indicated that there was no significant aggregation of nanotubes during the evaporation of chloroform. This is surprising considering the aggregates seen on the optical micrographs. As the SEM images suggest, the nanotubes in the aggregates are packed loosely and are not in a close contact with each other. This should allow the individual tubes to still reveal their absorption features.

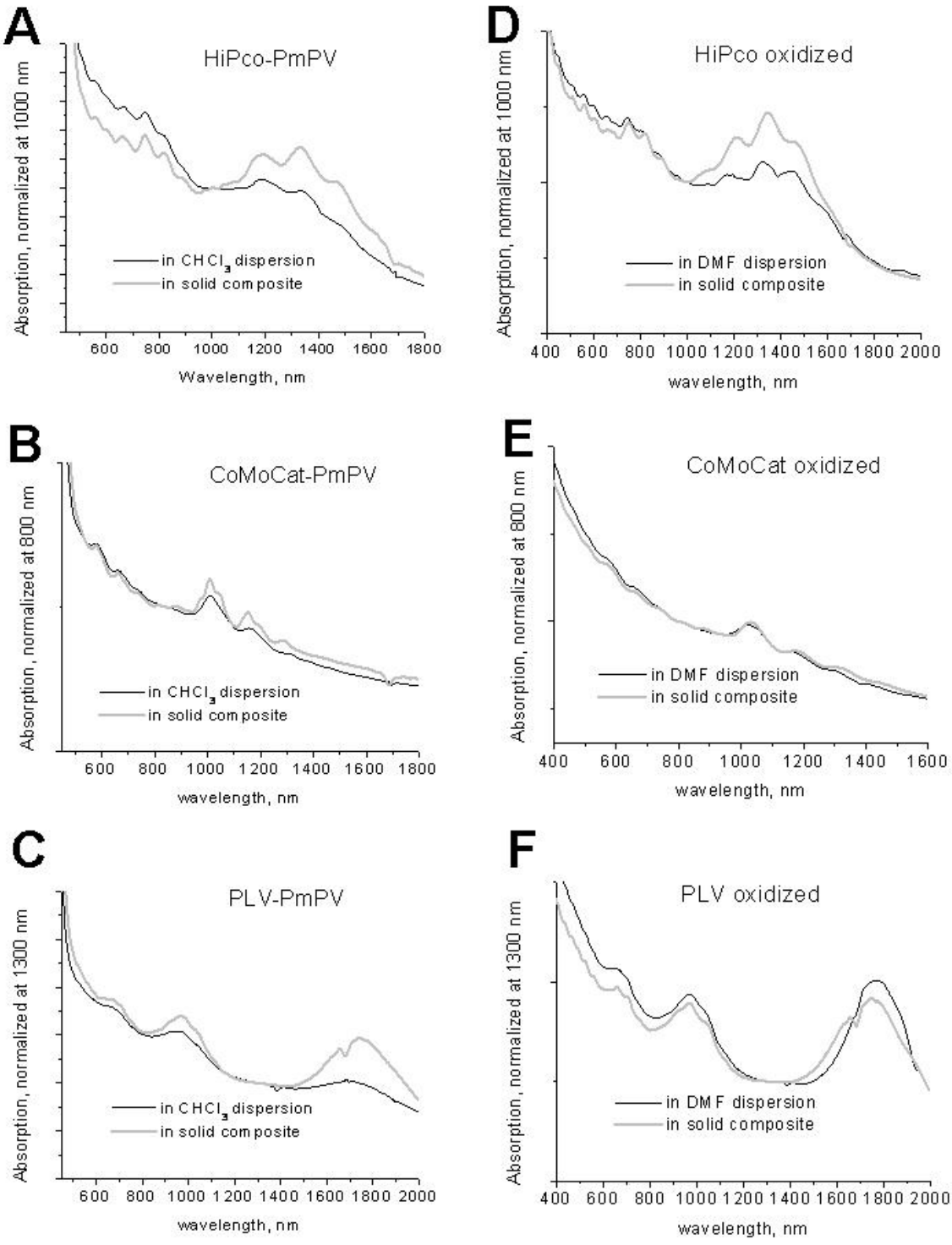

Figure 6. Optical absorption of the PmPV-functionalized SWNT in chloroform dispersions and in solid PS composites. A, D – HiPco, B, E - CoMoCat, C, F - PLV.

Composites of oxidized SWNT in polystyrene. We prepared composites of the oxidized SWNT and polystyrene by precipitation of DMF dispersions into water. Evaporation of the solvent failed for this material. Slow evaporation of DMF resulted in premature aggregation of nanotubes as the solution concentrated. Dry composite material obtained by precipitation appeared as agglomerates of small particles. Therefore the quality of mixing during the molding affected the conductivity results significantly. We have found that pressing the samples at 175 °C greatly increased their conductivity compared to pressing at 140 °C, presumably due to a better fusing of particles at higher temperature. Figure 7 shows the AFM images of the oxidized nanotubes deposited from the DMF dispersions and optical microscopy of the composite films containing 0.6 wt % of the same nanotubes.

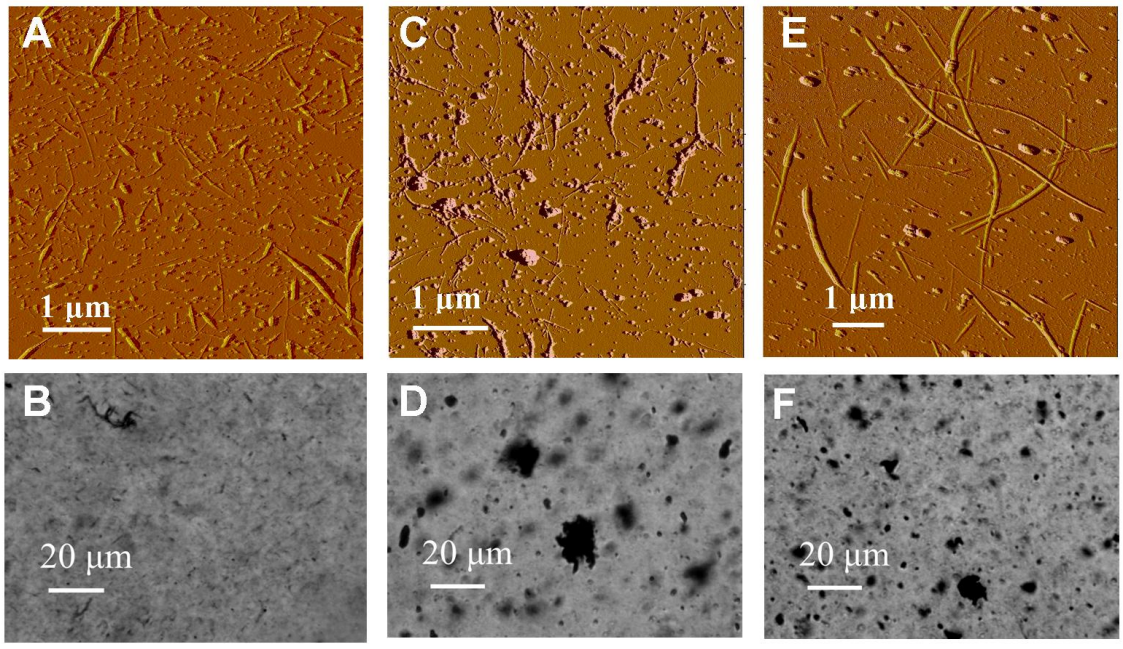

Figure 7. AFM of the oxidized SWNT and SEM of the composites of 0.6% SWNT in polystyrene. A, B – HiPco; C, D – CoMoCat; E, F – PLV.

The length and height distribution of bundles in the SWNT oxidized by 60 min of sonication in 8 M HNO_3 has been presented in Chapter IV (Figures 3 and 4). In the section analysis of the AFM images over 80% of tubular objects had heights 10 nm and less, but the average diameter was higher than that in the PmPV-functionalized samples. Small globular particles appeared on the AFM image of HiPco tubes compared to the pristine sample in Figure 2A and a certain increase in number of these particles for the oxidized CoMoCat sample suggest some accumulation of amorphous carbon after the oxidation procedure. The measurements of length revealed a moderate shortening of nanotubes compared to the PmPV dispersed materials that were subjected only to a brief sonication. Optical micrographs of the composites of oxidized SWNT looked very similar to those for the PmPV-functionalized composites, small tubular particles in HiPco composites and large globular agglomerates in CoMoCat and PLV composites werw observed. HiPco material was the most stable against aggregation regardless of the way the composite was prepared.

Optical absorption spectra of the coagulated composites, presented in Figure 6 (D, E, F), similar to the PmPV-functionalized material, did not show a decrease in the interband transition peaks intensities, which is an indicator that the coagulation procedure was not accompanied by a noticeable bundling of nanotubes. According to Itkis,[33] amorphous carbon accumulated in the material should decrease the relative area under the peaks, which was not the case for our slightly oxidized material, as can be judged by the UV-VIS spectra.

Electrical conductivity of the SWNT composites. Figures 8, 9 and 10 report electrical conductivity of the polystyrene composites of the SWNT materials studied in

this work. The results for the percolation threshold, as well as critical exponent β and prefactor C of the equation (1), are summarized in Table 2 and combined with the measurements of diameter and length of nanotubes obtained from AFM. The composites prepared with the aid of PmPV had a lower percolation threshold than the composites of oxidized nanotubes. These results don't correlate with SEM or optical microscopy. Instead, one should closely analyze the size of bundles measured by AFM.

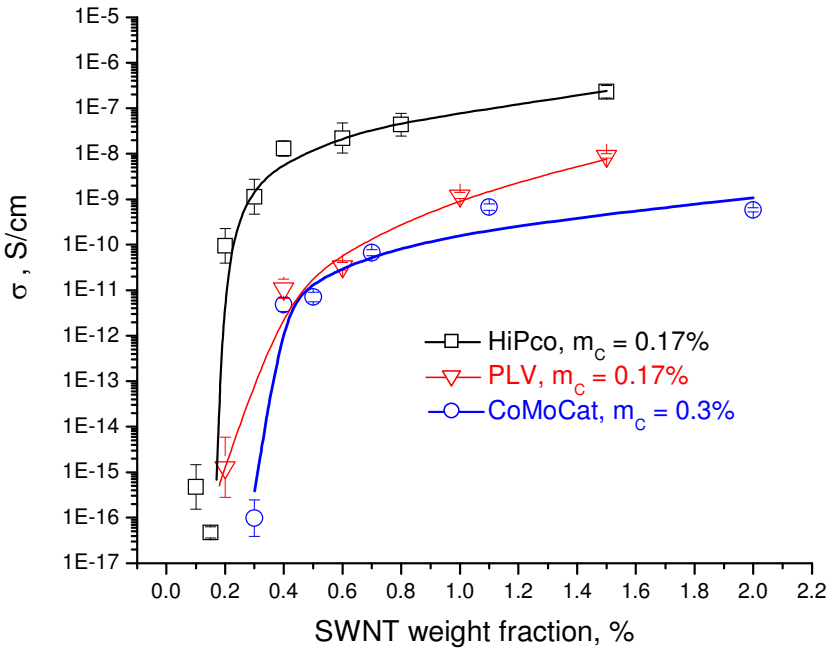

Figure 8. Electrical conductivity of the composites of SWNT in polystyrene with the presence of PmPV. Standard deviation was calculated with 95% confidence.

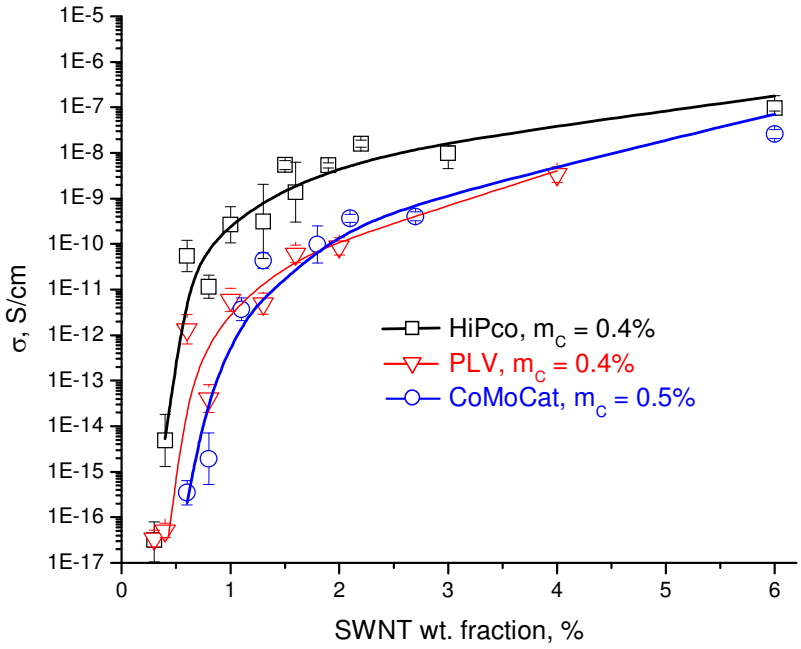

Figure 9. Electrical conductivity of oxidized SWNT in polystyrene.

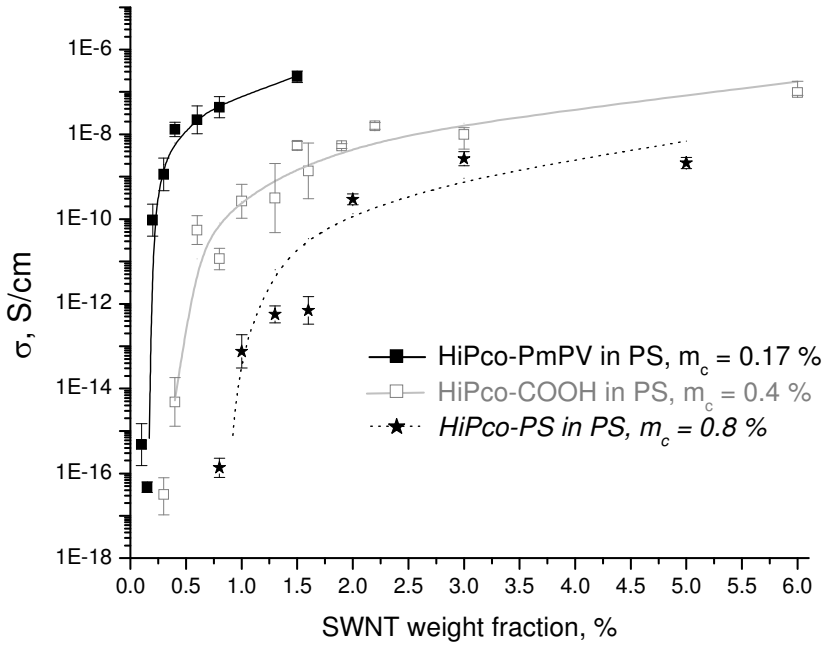

Figure 10. Electrical conductivity of the HiPco SWNT in PS.

Table 2. Size of nanotubes and calculated parameters for the equation $\sigma = C(m-m_c)^{\beta}$

SWNT	Average diameter d, nm	Average length L, nm	Aspect ratio, L/d	percolation threshold m_c, weight %	critical exponent β	prefactor C
HiPco-PmPV	3.2	734	230	0.17	2.0	$1.2*10^{-7}$
HiPco oxidized	4.4	540	122	0.4	2.9	$4.8*10^{-4}$
HiPco functionalized with PS	7.5	820	109	0.8	4.0	$1.9*10^{-3}$
CoMoCat-PmPV	3.1	690	223	0.3	2.0	$3.9*10^{-6}$
CoMoCat oxidized	4.2	620	148	0.5	4.8	$7.6*10^{-2}$
PLV-PmPV	4.6	1020	222	0.17	4.1	0.4
PLV oxidized	5.8	790	136	0.4	4.5	$8.8*10^{-3}$

According to the calculations, the percolation threshold in the system of conducting cylinders depends upon the aspect ratio of the cylinders.[34] The oxidized nanotubes have both a smaller aspect ratio and larger diameter of bundles than the PmPV dispersed materials. Consequently, the percolation threshold for oxidized SWNT is higher than that for the corresponding PmPV-wrapped nanotubes. However, there is no correlation between the aspect ratio and percolation threshold between different nanotube types within the series. HiPco and PLV materials have the same m_c value in each series regardless of the large aggregates on the optical micrographs of the PLV composites. CoMoCat material stands alone in having the higher percolation threshold. For this issue one should take in account differences the size of nanotubes in different materials. The average diameter of individual nanotubes is 0.8 nm for CoMoCat,[35] 1.0 nm for HiPco[36] and 1.3 for PLV.[37] A bundle of CoMoCat SWNT should contain more nanotubes than the bundle of HiPco or PLV SWNT of the same size, which makes the density of the

CoMoCat bundles higher. Since the percolation threshold is volume dependent while we are measuring mass, this will increase the mass fraction of this material needed for percolation. From this point of view, the PLV nanotubes should have the lowest density and the lowest m_c. Probably the noticeable fraction of the low aspect ratio amorphous carbon in the PLV sample suppresses its performance.

Comparison of the composites made from the HiPco SWNT processed by different methods shows that the sample covalently functionalized with polystyrene had the highest percolation threshold. The 2–fold increase in this factor compared to the oxidized SWNT does not correlate with only a 10% change in the aspect ratio of the nanotube bundles. Therefore, it is not the aspect ratio that is responsible for the higher percolation threshold of the PS-functionalized composites, but most probably the presence of the polystyrene chains permanently bound to the SWNT surface may prevent nanotubes from getting into a good contact between each other during the preparation of the composites. One may argue that the PmPV dispersed SWNT also should have a layer of the PmPV polymer at their surface in composites. However, this layer is not insulating. Electrical conductivity of neat PmPV is $2*10^{-12}$ S/cm,[21] which is 6 orders of magnitude higher than that of polystyrene. We presume that the density of the PS grafted to SWNT was low, as judged by Raman and TGA results in Chapter II B, so nanotubes can still come in contact. However, more nanotubes are required to build a continuous percolation network. Unfortunately, there are no data in the literature on electrical conductivity of the polymer grafted carbon nanotubes. Presumably, the dense coverage of the SWNT surface with an insulating polymer such as polystyrene should completely prevent the electrical current throughout the composite.

The critical exponent for the PmPV functionalized HiPco and CoMoCat nanotubes was 2.0, which is in a good agreement with the calculated value of 1.6 – 2.0.[3,4] The value for β reported in literature varies from 1.2[5] to 7.55[12] and is generally lower for the thin films obtained by solution casting (see Table 1). Kogut and Straley[38] have shown that the critical exponent can increase for the composite systems whose elements have a distribution of conductivity and its deviation from the theoretical value β_0 can be expressed by the formula:

$$\beta = \beta_0 + \alpha/(1-\alpha) \qquad (4)$$

where α is a parameter defining the distribution of conductivity. Vionnet-Menot[39] has proposed that α relates to the tube to tube electron transport efficiency. The nitric acid treatment that we utilized is known to introduce defects along the sidewalls[40] which should change electronic properties of nanotubes. Previously we have found that such changes increased in the row of PLV – HiPco – CoMoCat.[29] The highest degree of chemical functionalization of CoMoCat SWNT induced by oxidation should alter the electron transport properties of this material the most which was probably the reason for the biggest change in the value of β between the two series. According to our previous study,[29] the PLV SWNT was practically unaffected by the 60 min sonication in acid which can explain the smallest change in β for this material. In the series of composites made from different HiPco materials the higher critical exponent was found for the PS-functionalized samples, which is the result of increased tube to tube resistance as was explained by Vionnet-Menot.[39]

While the percolation threshold relates to the geometry of the nanotube bundles, the conductivity of the composites at the plateau region has to depend upon conductivity of the nanotube material itself. We have found that HiPco SWNT had the highest and CoMoCat – the lowest conductivity of the composites above the percolation threshold for both series. CoMoCat has a narrow distribution of nanotubes by type and contains about 9% of metallic SWNT by weight.[41] There are no such estimation for HiPco and PLV in literature. Presumably, HiPco material, having a large variety of different types of tubes,[42] contains more metallic tubes than CoMoCat and therefore should be more conductive.

Conclusions

The PmPV copolymer is a good stabilizing agent for organic dispersions of carbon nanotubes. Preparation of composites via rapid evaporation of the SWNT dispersions is more efficient method than coagulation. This technique eliminates the need for pre-treatment of nanotubes and allows the solvent recycling. The minimal damage of nanotubes during the evaporation method preserves the high aspect ratio allowing the lower percolation threshold. The main drawback of this method is the presence of the PmPV copolymer in the composites which may change the mechanical properties of the host polymer. The use of oxidized SWNT simplifies the composite content. However, the nitric acid treatment shortens the nanotubes, decreasing the aspect ratio. Our results show that the aspect ratio of nanotube bundles affects the percolation threshold value of the composites. We have found that the electrical conductivity at the plateau region depends

on the type of SWNT material, which we attribute to the differences in the fraction of the metallic nanotubes in these materials. This fraction is probably the highest in HiPco SWNT.

The exponent β as a factor related to the electron transport through the nanotubes was higher for the composites of oxidized SWNT due to the larger amount of the structural defects in the nanotubes as a result of nitric acid oxidation. Since the CoMoCat nanotubes are highly vulnerable to the oxidation, the increase in β for this material was the highest. The PLV nanotubes, being the most stable to the acidic treatment, expressed the smallest changes in the critical exponent. This phenomenon has been studied mostly theoretically, but more experimental results are needed to better explore the relations between the structure of SWNT and the exponent β in the composites.

The polystyrene functionalized HiPco nanotubes, despite a higher solubility and an ideal compatibility of the attached molecules with the host polymer, exhibited lower electrical conductivity compared to the SWNT processed by other two methods. Attached insulating polymer prevented contact and charge transfer between nanotubes, resulting in a lower electrical conductivity of the samples. Evidently, this technique should not be used for preparation of conductive polymeric composites of SWNT.

References

(1) Thess, A.; Lee, R.; Nikolaev, P.; Dai, H.; Petit, P.; Robert, J.; Xu, C.; Lee, Y. H.; Kim, S. G.; Rinzler, A. G.; Colbert, D. T.; Scuseria, G. E.; Tomanek, D.; Fischer, J. E.; Smalley, R. E. *Science* **1996**, *273*, 483.

(2) Benoit, J.-M.; Corraze, B.; Lefrant, S.; Blau, W. J.; Bernier, P.; Chauvet, O. *Synth. Met.* **2001**, *121*, 1215.

(3) Stauffer, D.; Aharony, A.; *Introduction to Percolation Theory*; 2nd ed.; Taylor and Francis: London, 1994.

(4) Straley, J. P. *Ann. of Isr. Phys. Soc.* **1983**, *5*, 353.

(5) Sandler, J. K. W.; Kirk, J. E.; Kinloch, I. A.; Shaffer, M. S. P.; Windle, A. H. *Polymer* **2003**, *44*, 5893.

(6) Bryning, M. B.; Islam, M. F.; Kikkawa, J. M.; Yodh, A. G. *Adv. Mater.* **2005**, *17*, 1186.

(7) Ramasubramaniam, R.; Chen, J. *Appl. Phys. Lett.* **2003**, *83*, 2928.

(8) Gojny, F. H.; Wichmann, M. H. G.; Fiedler, B.; Kinloch, I. A.; Bauhofer, W.; Windle, A. H.; Schulte, K. *Polymer* **2006**, *47*, 2036.

(9) Ounaies, Z.; Park, C.; Wise, K. E.; Siochi, E. J.; Harrison, J. S. *Composite Sci. Tech.* **2003**, *63*, 1637.

(10) Jiang, X.; Bin, Y.; Matsuo, M. *Polymer* **2005**, *46*, 7418.

(11) Skakalova, V.; Dettlaff-Weglikowska, U.; Roth, S. *Synthetic Metals* **2005**, *152*, 349.

(12) Ha, M. L. P.; Grady, B. P.; Lolli, G.; Resasco, D. E.; Ford, W. T. *Macromol. Chem. Phys.* **2007**, *208*, 446.

(13) Nogales, A.; Broza, G.; Roslaniec, Z.; Schulte, K.; Sics, I.; Hsiao, B. S.; Sanz, A.; Garcia-Gutierrez, M. C.; Rueda, D. R.; Domingo, C.; Ezquerra, T. A. *Macromolecules* **2004**, *37*, 7669.

(14) Chang, T.-E.; Kisliuk, A.; Rhodes, S. M.; Brittain, W. J.; Sokolov, A. P. *Polymer* **2006**, *47*, 7740.

(15) Grossiord, N.; Miltner, H. E.; Loos, J.; Meuldijk, J.; Van Mele, B.; Koning, C. E. *Chem. Mater.* **2007**, *19*, 3787.

(16) Du, F.; Fischer, J., E.; Winey, K. I. *J. Polym. Sci.: B.* **2003**, *41*, 3333.

(17) Hornbostel, B.; Potschke, P.; Kotz, J.; Roth, S. *Phys. Stat. Sol. B.* **2006**, *243*, 34453451.

(18) Seo, M.-K.; Park, S.-J. *Chem. Phys. Lett.* **2004**, *395*, 44.

(19) Gorrasi, G.; Sarno, M.; Di Bartolomeo, A.; Sannino, D.; Ciambelli, P.; Vittoria, V. *J. Polym. Sci.: B:* **2007**, *45*, 597.

(20) McNally, T.; Potschke, P.; Halley, P.; Murphy, M.; Martin, D.; Bell, S. E. J.; Brennan, G. P.; Bein, D.; Lemoine, P.; Quinn, J. P. *Polymer* **2005**, *46*, 8222.

(21) Coleman, J. N.; Curran, S.; Dalton, A. B.; Davey, A. P.; McCarty, B.; Blau, W.; Barklie, R. C. *Phys. Rev. B* **1998**, *58*, 7492.

(22) Dai, H.; Rinzler, A. G.; Nikolaev, P.; Thess, A.; Colbert, D. T.; Smalley, R. E. *Chem. Phys. Lett.* **1996**, *260*, 471.

(23) Kityanan, B.; Alvarez, W. E.; Harwell, J. H.; Resasco, D. E. *Chem. Phys. Lett.* **2000**, *317*, 497.

(24) Arepalli, S.; Nikolaev, P.; Holmes, W.; Files, B. S. *Appl. Phys. Lett.* **2001**, *78*, 1610.

(25) Star, A. J.; Stoddart, F.; Steuerman, D.; Diehl, M.; Boukai, A.; Wong, E. W.; Yang, X.; Chung, S.-W.; Choi, H.; Heath, J. R. *Angew. Chem. Int. Ed.* **2001**, *40*, 1721.

(26) Chen, J.; Liu, H.; Weimer, W. A.; Halls, M. D.; Waldeck, D. H; Walker, G. C. *J. Am. Chem. Soc.* **2002**, *124*, 9034.

(27) Matarredona, O.; Rhoads, H.; Li, Z.; Harwell, J. H.; Balzano, L.; Resasco, D. E. *J. Phys. Chem. B* **2003**, *107*, 13357.

(28) Gorelik, O. P.; Sosa, E.; Nikolaev, P.; Holmes, W.; Arepalli, S.; Yowell, L. *232nd ACS National Meeting*: San Francisco, CA, 2006, Presidential Symposium.

(29) Tchoul, M. N., Ford, W. T.; Lolli, G.; Resasco, D. E.; Arepalli, S. *Chem. Mater.* **2007**, *19*, 5765.

(30) Lipatov, Y. S.; Sergeeva, L. M *Adsorption of Polymers*; John Wiley & Sons, LTD: New York, 1974.

(31) Loos, J.; Alexeev, A.; Grossiord, N.; Koningc, C. E.; Regev, O. *Ultramicroscopy* **2005**, *104*, 160.

(32) Reich, S.; Thomsen, C.; Ordejon, P. *Phys. Rev. B* **2002**, *65*, 155411/1.

(33) Itkis, M. E.; Perea, D. E.; Niyogi, S.; Rickard, S. M.; Hamon, M. A.; Hu, H.; Zhao, B.; Haddon, R. C. *Nano Lett.* **2003**, *3*, 309.

(34) Munson-McGee, S. H. *Phys. Rev. B* **1991**, *43*, 3331.

(35) Bachilo, S. M.; Balzano, L.; Herrera, J. E.; Pompeo, F.; Resasco, D. E.; Weisman, R. B. *J. Am. Chem. Soc.* **2003**, *125*, 11186.

(36) Zhou, W.; Ooi, Y. H.; Russo, R.; Papanek, P.; Luzzi, D. E.; Fischer, J. E.; Bronikowski, M. J.; Willis, P. A.; Smalley, R. E. *Chem. Phys. Lett.* **2001**, *350*, 6.

(37) Yudasaka, M.; Sensui, N.; Takizawa, M.; Bandow, S.; Ichihashi, T.; Iijima, S. *Chem. Phys. Lett.* **1999**, *312*, 155.

(38) Kogut, P. M.; Straley, J. P. *J. Phys. C* **1979**, *12*, 2151.

(39) Vionnet-Menot, S.; Grimaldi, C.; Maeder, T.; Strassler, S.; Ryser, P. *Los Alamos National Laboratory, Preprint Archive, Condensed Matter* **2005**, 1.

(40) Zhang, J.; Zou, H.; Qing, Q.; Yang, Y.; Li, Q.; Liu, Z.; Guo, X.; Du, Z. *J. Phys. Chem. B* **2003**, *107*, 3712.

(41) Jorio, A.; Santos, A. P.; Ribeiro, H. B.; Fantini, C.; Souza, M.; Vieira, J. P. M.; Furtado, C. A.; Jiang, J.; Saito, R.; Balzano, L.; Resasco, D. E.; Pimenta M. A. *Phys. Rev. B* **2005**, *72*, 075207/1.

(42) Bachilo, S. M.; Strano, M. S.; Kittrell, C.; Hauge, R. H.; Smalley, R. E.; Weisman, R. B. *Science* **2002**, *298*, 2361.

CHAPTER VI

CONCLUDING REMARKS

In this work different methods of dispersing carbon nanotubes in solvents were studied. Moreover, investigations were made on the mild nitric acid oxidation, covalent functionalization with polystyrene, and non-covalent functionalization with poly(phenylene vinylene). Effects of the physical properties of different SWNT materials on the electrical properties of the resulting polystyrene composites were studied. Length and diameter of the nanotube bundles, degree of functionalization of SWNT, functional groups on the surface of nanotubes, tube-to-tube contact, and ratio of metallic to semiconducting tubes in the material affected the properties of the nanotube containing composites. A lower aspect ratio of the oxidized SWNT due to the oxidative shortening resulted in a higher percolation threshold for the electrical conductivity of the composites. Covalent attachment of polystyrene to SWNT reduced the conductivity of the composites since the polymer chains immobilized on the nanotube surface prevented sufficient contact between tubes. A higher fraction of metallic tubes in HiPco material led to a higher conductivity of the corresponding polystyrene composites compared to those made with other SWNT materials.

Since such properties as mechanical strength, chemical reactivity and electron transport are strongly dependent on the specific chirality and diameter of nanotubes, there is a tube type which ultimately defines the properties of the composite material.

This correlation seems evident, although it is not often taken in account, especially in the area of Material Science and Engineering, as a study of the literature reveals. Every synthetic method for producing of SWNT results in a mixture of tens of different types of tubes, while a large scale separation technique is not available. Carbon nanotube materials produced by different methods are composed of the same types of tubes, but in different proportions, not to mention variations in length, which accounts for differences in the properties of these materials. In this work it was shown that for the development of new nanotube-enabled materials, the content of the SWNT sample is a very important factor to consider. If high electrical conductivity of the composite is a goal, the sample with a high fraction of metallic nanotubes is preferable. If carboxylic groups are to be created on the SWNT for further functionalization, the oxidation protocol has to be mild for the sample where small tubes prevail, since the same conditions may moderately oxidize one SWNT material and completely destroy another. If mechanical reinforcement is sought, longer nanotubes will give the greater effect.

Moreover, the very term “carbon nanotubes”, similar to such terms as “alkanes” or “waxes”, has to be interpreted not as a certain chemical compound but as a class of compounds that possess both mutual and structurally dependent chemical properties. As the present work clearly shows, such an understanding is important not only in the physics of carbon nanotubes but in all other areas of carbon nanotube science and technology.

VITA

Maxim Nikolaevich Tchoul

Candidate for the Degree of

Doctor of Philosophy

Thesis: COMPOSITES OF CARBON NANOTUBES

Major Field: Chemistry

Biographical:

Personal Data: Born in Murmansk, Russia, on September 6, 1969.

Education: Graduated from Mozyr High School No 10, Mozyr, Belarus in June 1986; received Diploma (equivalent of Master of Science) in Chemistry from Belarus State University, Minsk, Belarus in June 1992; completed the requirements for the Doctor of Philosophy in Chemistry at Oklahoma State University, Stillwater, Oklahoma in May, 2008.

Experience: Research Engineer, Institute for Physical Organic Chemistry of National Academy of Science of Belarus, Minsk, Belarus 1992-1995. Technologist, Korpack Co, Minsk, Belarus 1995-1997. Production Manager, Deltaplastic Ltd., Minsk, Belarus 1997-2002. Research Assistant, Department of Chemistry, Oklahoma State University, Stillwater, Oklahoma, 2003-2008.

Professional Memberships: American Chemical Society, Oklahoma Microscopy Society.

Name: Maxim Nikolaevich Tchoul Date of Degree: May, 2008

Institution: Oklahoma State University Location: Stillwater, Oklahoma

Title of Study: COMPOSITES OF CARBON NANOTUBES

Pages in Study: 102 Candidate for the Degree of Doctor of Philosophy

Major Field: Chemistry

Scope and Method of Study: The purpose of this research was to study various methods of incorporation of single-walled carbon nanotubes (SWNT) with polymers for producing electrically conductive polystyrene composites. SWNT of three different types were dispersed in solvents by noncovalent "wrapping" with a semiconjugated copolymer, nitric acid oxidation, and covalent grafting with both polystyrene and poly(vinylbenzyl trimethylammonium chloride). Composites were prepare via solution mixing. Effect of the type of SWNT material and the preparation method on electrical conductivity of the resulting composites was investigated.

Findings and Conclusions: Covalent grafting of SWNT with poly(vinylbenzyl trimethylammonium chloride) gave stable dispersions of carbon nanotubes in water and produced polymeric composites via layer-by-layer deposition. Grafting of polystyrene increased dispersability of SWNT in organic solvents. Mild nitric acid oxidation of carbon nanotubes also resulted in stable dispersions of SWNT in DMF, methanol, and water. Mixing SWNT and polystyrene in DMF or chloroform solutions, followed by rapid removing of solvent via either precipitation in water or evaporation under vacuum, resulted in composites with uniform distribution of carbon nanotube bundles. Electrical conductivity of these composites was dependent on the physical properties of bundles of the SWNT such as aspect ratio, density, fraction of metallic nanotubes, chemical functionalization, and presence of the molecules immobilized at the surface.